THE ASTROPHYSICAL JOURNAL, 354:310–332, 1990 May 1

LITHIUM DEPLETION AND ROTATION IN MAIN-SEQUENCE STARS

SUCHITRA BALACHANDRAN
Department of Astronomy, The University of Texas at Austin
Received 1989 June 26; accepted 1989 November 1

ABSTRACT

Lithium abundances were measured in nearly 200 old disk-population F stars to examine the effects of rotational braking on the depletion of Li. The sample was selected to be slightly evolved off the main sequence so that the stars have completed all the Li depletion they will undergo on the main sequence. We find a large scatter in Li abundances in the late F stars, indicating that the Li depletion is not related to age and spectral type alone. Conventional depletion mechanisms like convective overshoot and microscopic diffusion are unable to explain Li depletion in F stars with thin convective envelopes and are doubly taxed to explain such a scatter. No correlation is found between Li abundance and the present projected rotational velocity, $v \sin i$, and some of the most rapid rotators are undepleted, ruling out meridional circulation as the cause of Li depletion. There is a somewhat larger spread in Li abundances in the spun-down late F stars compared to the early F stars which should remain rotationally unaltered on the main sequence. We suggest that Li depletion may occur as a result of mixing induced by differential rotation when a rapidly rotating star spins down on the main sequence. The range in Li abundance would then result from an initial range in rotational velocities. Contrary to earlier understanding, some Li depletion is seen in a few early F stars which have evolved from main-sequence effective temperatures greater than 7000 K. Highly Li depleted stars with upper limit estimates of $\log \epsilon(\mathrm{Li}) < 2.0$ are clumped in the H-R diagram and are identified as slightly evolved Li "dip" stars. This clump is not coincident with the rotational break seen in the main sequence but is at the upper end of stars which have slowed down. To first approximation, "dip" stars of all metallicities have evolved from the same main-sequence temperature interval; the metal-poor "dip" stars have smaller masses than the solar metallicity stars.

Subject headings: stars: abundances — stars: rotation

I. INTRODUCTION

Stars are formed with a Li abundance $\log \epsilon(\mathrm{Li}) \sim 3.0$ [on the scale where $\log \epsilon(\mathrm{H}) = 12.0$] as evidenced from observations of early Population I stars, the interstellar medium, and meteoritic samples. At the beginning of this decade, the pattern of Li depletion in main-sequence stars seemed fairly well understood. It was observed that early F stars retained the Li with which they were formed, while later type G and K stars, with deeper convective envelopes, showed evidence of Li depletion (Herbig 1965; Wallerstein, Herbig, and Conti 1964). That Li depletion took place on the main sequence became clear from comparisons of the Hyades and the Pleiades; the older Hyades stars had less Li than Pleiades stars at the same effective temperature (Zappala 1972). Early in the study of Li depletion, Weymann and Sears (1965) had calculated that the surface convection zones in late-type stars were not deep enough to destroy Li and, since then, "extra-mixing" mechanisms have been sought to take the surface material below the convection zone.

Most of the observational conclusions about the Li depletion pattern in main-sequence stars were based on studies of the Hyades, the closest and hence the best studied of all the open clusters. Echelle spectrographs and CCD detectors have made more distant clusters accessible, and it now appears that conclusions based on the Hyades observations may have distorted our understanding of Li depletion. The Hyades is the only cluster that shows a tight and well-defined Li abundance sequence with effective temperature. The large spread in Li abundances in stars at the same effective temperature was first seen in the Pleiades (Duncan and Jones 1983) and interpreted as being caused by an age spread in the formation of the cluster. A similar large spread in Li abundances was reported in a second young cluster, α Per (Balachandran, Lambert and Stauffer 1988, hereafter BLS). In clusters around the age of the Hyades, Coma (Boesgaard 1987*a*) and UMa (Boesgaard, Budge, and Burck 1988), some scatter is reported, but there is uncertainty in the cluster membership. In other older clusters, NGC 752 (Hobbs and Pilachowski 1986*a*; Pilachowski and Hobbs 1988) and NGC 188 (Hobbs and Pilachowski 1988), there are considerably fewer stars and greater membership uncertainties, making the observed scatter somewhat uncertain. However, recent observations may indicate that the scatter in Li abundances persists in M67 (Hobbs and Pilachowski 1986*b*; Garcia Lopez, Rebolo, and Beckman 1988). While the scatter in young clusters may be dismissed as being due to an age spread in the cluster, the persistence of the scatter in older clusters, if real, indicates that Li depletion is not a function of age and spectal type alone.

The modeling of the rotational history of the Sun from the Hayashi track to the present by Endal and Sofia (1981) was the first detailed study of the spinning down of a rapidly rotating star on the main sequence and revealed that mixing may occur down to depths where the material is expected to be completely Li depleted. More recent calculations (Pinsonneault *et al.* 1989) have extended this approach and are able to reproduce the observed Li depletion in the Sun. Observational evidence for a correlation between Li abundance and rotational velocity was first presented by Butler *et al.* (1987) for eight stars in the Pleiades; the rapid rotators had an order of magnitude larger abundance than the slow rotators. It was argued that this correlation in the Pleiades simply reflected the spread in the age of the cluster; the rapid rotators were younger stars. Observations of a larger sample of F, G, and K stars in the α Per cluster (BLS) showed that, while all the rapid rotators had their primordial Li abundance and the Li depleted stars were all slow rotators, not all the slow rotators were Li depleted. A correlation similar to that seen in the Pleiades has been reported in IC 2391 (Stauffer *et al.* 1989). In young clusters, the effects of the rotational braking and the age spread on the depletion of Li are clearly meshed and, since the extent of the latter is not well known, the effects of the former cannot be isolated.

To understand the effects of rotational braking on the depletion of Li, we examined a large sample of old disk-population field F stars taken from Eggen (1973). Age differences were minimized by choosing stars which were slightly evolved off the main sequence. This also ensured that the stars had completed all the Li depletion they would undergo on the main sequence. The stars have not evolved far enough toward the giant branch for the convective envelopes to have deepened and caused significant mixing (Iben 1967). By choosing F stars, we maximized the range in rotational velocity. Typically, early F stars are rapid rotators, while late F stars have been spun down by winds and magnetic fields. The stars are in the field and since they are not associated with any star-forming region, gas, dust, or unusual chromospheric emission, it can be reasonably assumed that they are not pre–main-sequence stars. We present here the results of this study.

II. OBSERVATIONS

Out of the 250 stars contained in Eggen's (1973) sample, 199 were observed (see Table 1). All the stars are contained in the *Bright Star Catalogue* (Holfleitt 1982, hereafter BSC). Most of the observations were carried out at the 2.1 m telescope at McDonald Observatory with the coudé spectrograph and, primarily, the Reticon detector (Vogt, Tull, and Kelton 1978) during seven observing runs between 1984 October and 1986 July. The spectra were obtained using a 12,000 lines mm^{-1} grating blazed at 6000 Å. A spectral coverage of about 120 Å was obtained with the 1728 element Reticon detector, each pixel in the detector being 15 μm wide. A slit width of 60 μm which projects onto two diodes was used under normal seeing conditions ($\sim 2''$) and a 3–4 diode slit if conditions were worse or if the star was a rapid rotator. Hence spectral resolutions vary between 0.14 and 0.28 Å. The spectra are centered around the 6707.8 Å Li I resonance doublet and include several Fe I lines. Typical integration times varied between a few minutes for a 3.0 mag star and 90 minutes for a 6.5 mag star. Typical signal-to-noise (S/N) ratios were ~ 100, though higher S/N ratios were obtained for the broad-lined rapid rotators. Spectra in the final observing run were obtained using a 512 × 512 RCA CCD detector array. With 30 μm pixels, the spectral coverage obtained with this detector was about 70 Å. Solar spectra were obtained with each detector by recording a sky spectrum during the day and used in the $v \sin i$ calibration (see § III*b*). About 25 southern stars were observed at a two-diode spectral resolution of 0.13 Å by D. L. Lambert and A. C. Danks using the ESO 1.4 m coudé auxiliary telescope at La Silla with a Reticon detector. The characteristics of the spectrometer are described in Enard and Anderson (1978) and Anderson (1980). Subscript "c" is used to denote spectra obtained with the CCD detector and subscript "e" is used for stars observed at ESO (Table 1). Sample spectra are illustrated in Figure 1. Broad-lined spectra of two rapid rotators are shown along with the synthetic fits made to them.

III. REDUCTION AND ANALYSIS

a) Equivalent Widths

Each stellar spectrum was divided by a flat-field spectrum to remove diode-to-diode variations. The wavelength scale was established by cross-correlating the spectrum with a narrow-lined, high S/N ratio reference spectrum in which several atomic lines had been identified. Next, the continuum was set and equivalent widths of the Li I feature and several Fe I lines were measured in the narrow-lined stars (see Table 1). Repeated settings of the continuum and measurements of equivalent widths indicated that errors in the measurement were less than 2 mÅ. Measurements of equivalent widths from two spectra of the same star yield differences of about 5 mÅ (e.g., compare equivalent widths from McDonald Reticon and ESO Reticon spectra in Table 1). Abundances of the broad-lined, rapidly rotating stars were determined through spectrum synthesis (see § III*c*).

The equivalent width of the Fe I (6707.4 Å) blend in the Li I feature was estimated from the measured equivalent widths of three other Fe I lines at λλ6705.105, 6726.67, and 6752.716 using the standard curve-of-growth technique. All three lines have the same excitation potential ($\chi = 4.6$ eV) as the 6707.4 Å Fe I blend. The average of the three equivalent widths obtained was adopted as the strength of the blend and subtracted from the measured equivalent width of the Li I feature to give the equivalent width of the Li I component alone. Typically, the Fe I blend had an equivalent width between 1 and 6 mÅ.

The 6707 Å Li feature is a doublet split by fine structure. In an attempt to speed up the analysis of our large sample of stars, we assumed that the Li feature was a single line with a *gf*-value equal to the sum of the *gf*-values of the component lines and used the program LINES (a derivative of MOOG; Sneden 1973) to calculate abundances from input equivalent widths and model atmospheres. However, to treat the Li feature as a single line, a correction must be applied to the measured equivalent width. For this calculation, we assumed that the Li I feature consisted of two lines at 6707.761 Å and 6707.912 Å with *gf*-values of 0.989 and 0.494, respectively (Andersen, Gustafsson, and Lambert 1984). The blended feature was then at 6707.811 Å (weighted average) with a *gf*-value (equal to the sum of the *gf*'s) of 1.483. Li abundances were first determined for input equivalent widths between 2 and 150 mÅ by taking the Li I feature as a single line with a *gf*-value of 1.483. Next, synthetic spectra of the Li feature were produced for various Li abundances with the feature taken as a blend of two lines with *gf*-values of 0.989 and 0.494, and the equivalent width of the feature was measured for each input abundance. A relation between the equivalent widths obtained by both techniques for the same abundance value was set up and used to change the measured equivalent width, $W_{0.494+0.989}$, to the corrected value $W_{1.483}$ so that the Li feature could be treated as a single line. While the correction is negligible at small equivalent widths, at 100 mÅ, the correction to the equivalent width is nearly 20 mÅ. The calibration was checked by determining the Li abundance of several narrow-lined stars through the calibration and by a synthetic fit and the agreement was found to be excellent. This is a relation between equivalent widths and is independent of the effective temperature of the star and any model atmosphere parameters. This calibration was merely

TABLE 1

EQUIVALENT WIDTHS, STELLAR PARAMETERS, AND ABUNDANCES

HR	Equivalent Widths (mÅ) Fe						Li	Effective Temperature (K)			log g		ξ[a]	v sin i[a]	M_V	log ε(Li)	[Fe/H]	[Fe/H]
	6678	6703	6705	6726	6750	6752	6707	(β)	(b-y)	Mean	(β)	(b-y)					phot	spec
17	92	14	21	24	43	22	24	6041	6102	6071	4.18	4.17	1.6	6	3.71	2.27	-0.37	-0.41±0.09
33	85	8	16	16	44	15	28	6064	6141	6102	4.13	4.12	1.6	6	3.58	2.35	-0.47	-0.58±0.08
33[e]	...	14	23	22	...	...	34	...	...	...	...	...	...	...	...	...	...	...
82[s]	...	...	...	...	...	...	49	6472	6469	6471	3.84	3.84	2.1	44	2.16	2.95	-0.00	-0.09
115[s]	...	...	...	...	...	...	34	6715	6656	6685	4.16	4.17	1.8	29	2.85	2.90	-0.08	-0.17
143	93	11	23	17	49	24	<8	6263	6296	6279	3.90	3.89	2.0	7	2.69	<1.97	-0.42	-0.28±0.10
145	97	24	29	37	55	20	19	6041	6101	6071	4.12	4.11	1.6	6	3.55	2.18	-0.34	-0.23±0.11
297[s]	...	...	...	...	...	...	9	6041	6089	6065	3.86	3.85	2.0	40	2.70	1.84	-0.01	-0.17
407[sb]	...	...	...	...	...	...	83	6453	6440	6446	3.87	3.87	2.1	27	2.30	3.18	-0.13	-0.21
409	101	17	25	26	48	15	<3	6041	6097	6069	4.05	4.04	1.7	6	3.33	<1.30	-0.28	-0.35±0.05
458[b]	102	27	33	38	65	36	25	6198	6198	6198	4.22	4.22	1.6	8	3.55	2.39	0.03	-0.03±0.13
463[s]	...	...	...	...	...	...	<1	6834	6763	6798	4.05	4.06	2.0	110	2.49	<1.50	-0.27	-0.47
518[s]	...	...	...	...	...	...	85	6355	6353	6354	3.91	3.91	2.0	27	2.57	3.20	-0.24	-0.05
523	116	20	28	33	58	30	41	6087	6097	6092	4.33	4.33	1.4	5	4.04	2.53	-0.14	-0.18±0.05
544[sb]	...	...	...	...	...	...	<3	6284	6292	6288	3.91	3.91	2.0	100	2.62	<1.50	-0.16	0.00
593[sc]	...	...	...	...	...	...	<5	6519	6476	6497	4.14	4.14	1.8	25	2.99	<1.85	-0.11	-0.12
635	122	49	48	47	96	53	14	6154	6176	6165	4.00	4.00	1.8	9	2.97	2.08	0.09	0.36±0.20
638	87	13	19	14	35	14	3	6581	6542	6562	4.05	4.06	1.9	6	2.68	<1.69	-0.09	-0.23±0.08
646	94	15	28	23	45	19	75	6385	6370	6378	4.08	4.09	1.8	8	3.06	3.08	-0.38	-0.18±0.05
650	93	22	41	43	57	41	47	6087	6107	6097	4.15	4.15	1.6	12	3.52	2.61	-0.08	-0.11±0.19
657	124	17	35	39	55	27	<4	6304	6294	6299	4.12	4.12	1.7	15	3.21	<1.60	-0.23	0.02±0.07
673[c]	...	11	17	20	34	15	61	6345	6338	6342	3.99	3.99	1.9	15	2.78	2.90	-0.20	-0.40±0.05
728[c]	...	...	...	...	...	...	82	6675	6641	6658	4.05	4.06	1.9	60	2.56	3.25	0.00	0.09
740	89	14	21	21	38	11	81	6345	6345	6345	4.00	4.00	1.9	7	2.84	3.04	-0.34	-0.30±0.07
740[e]	...	12	21	22	...	...	80	...	...	...	...	...	...	...	...	...	...	...
756[s]	...	...	...	...	...	...	<7	6325	6313	6319	4.08	4.09	1.8	27	3.05	<1.87	-0.10	-0.05
761	101	15	34	24	46	19	<3	6110	6154	6132	4.02	4.02	1.8	6	3.18	<1.34	-0.29	-0.33±0.08
770	102	23	31	23	38	13	68	6491	6461	6476	4.02	4.02	1.9	16	2.69	3.10	-0.13	-0.08±0.16
781[b]	87	8	20	23	45	21	28	6444	6402	6423	4.22	4.23	1.6	8	3.33	2.59	-0.14	-0.28±0.09
863[sc]	...	...	...	...	...	...	10	6555	6544	6549	4.02	4.02	1.9	25	2.57	2.20	0.10	0.03
869[b]	90	16	20	21	41	20	<8	6395	6364	6380	4.17	4.17	1.7	15	3.22	<2.03	-0.14	-0.23±0.10
870	114	27	51	36	60	30	8	6519	6524	6521	4.11	4.11	1.8	9	2.85	2.10	0.17	0.23±0.09
934[s]	...	...	...	...	...	...	43	6841	6789	6815	4.01	4.02	2.0	75	2.33	3.10	-0.13	-0.44
963	93	19	25	26	47	21	18	6143	6161	6152	4.15	4.15	1.6	7	3.49	2.24	-0.22	-0.27±0.08
975	80	7	14	26	34	21	47	6666	6612	6639	3.99	3.99	2.0	20	2.47	2.99	-0.31	-0.23±0.13
1069[s]	...	...	...	...	...	...	81	6641	6588	6615	4.06	4.07	1.9	34	2.68	3.20	-0.22	0.03
1071	102	29	33	40	52	24	<1	6187	6197	6192	4.15	4.15	1.6	5	3.44	<0.93	-0.24	-0.10±0.12
1257	112	29	28	41	55	30	67	6231	6235	6233	4.04	4.04	1.8	6	3.04	3.01	-0.09	-0.04±0.11

TABLE 1—*Continued*

HR	Equivalent Widths (mÅ) Fe 6678	6703	6705	6726	6750	6752	Li 6707	Effective Temperature (K) (β)	(b-y)	Mean	log g (β)	(b-y)	ξ^a	v sin i[a]	M_V	log ε(Li)	[Fe/H] phot	[Fe/H] spec
1406[sb]	...	...	...	...	...	...	13	6143	6177	6160	3.85	3.84	2.0	33	2.57	2.08	-0.07	-0.10±0.10
1538	111	23	40	35	66	30	<5	6291	6126	6209	4.09	4.11	1.7	8	3.14	<1.65	0.05	-0.01±0.05
1545	80	6	20	16	31	8	24	6209	6234	6222	4.15	4.15	1.7	5	3.48	2.37	-0.42	-0.62±0.09
1822[s]	...	...	...	...	...	...	40	6143	6207	6175	3.68	3.67	2.3	43	2.14	2.61	-0.29	-0.07
1828	123	32	50	41	65	35	16	5872	5958	5915	3.98	3.97	1.8	5	3.27	1.94	-0.15	-0.08±0.10
1935	116	10	27	27	60	27	29	6335	6332	6334	3.94	3.94	2.0	29	2.63	2.53	-0.09	-0.11±0.15
2085	75	13	7	16	32	23	37	6976	6902	6939	4.23	4.24	1.8	16	2.84	3.08	-0.17	-0.13±0.23
2186	86	8	20	18	48	24	<8	6434	6408	6421	4.11	4.11	1.8	17	2.99	<2.01	-0.04	-0.28±0.14
2186[e]	...	14	28	34	0..	0..	<4	...	...	...	...	...	...	...	...	...	...	...
2264[b]	112	20	29	30	55	23	115	6754	6816	6785	3.95	3.94	2.1	11	2.11	3.76	0.30	0.27±0.13
2313	112	23	33	34	61	24	37	6041	6072	6056	4.17	4.17	1.6	6	3.64	2.49	-0.15	-0.16±0.03
2313[e]	...	23	35	38	...	...	43	...	...	...	...	...	...	...	...	...	...	...
2530	92	5	16	14	30	23	1	6491	6453	6472	4.17	4.18	1.7	10	3.22	<1.07	-0.47	-0.35±0.15
2601	98	12	19	24	45	20	4	5885	6050	5968	4.05	4.03	1.7	5	3.59	<1.34	-0.57	-0.49±0.07
2740[sc]	...	...	...	...	...	...	43	6875	6817	6846	4.13	4.14	1.9	50	2.63	3.10	-0.10	-0.37
2832	96	13	23	19	48	18	31	6453	6424	6439	4.06	4.06	1.9	14	2.89	2.65	-0.32	-0.21±0.06
2906	101	20	41	28	47	18	<2	6325	6309	6317	4.11	4.11	1.7	7	3.15	<1.34	-0.17	-0.10±0.10
2906[e]	...	20	26	28	...	...	<5	...	...	...	...	...	...	...	...	...	...	...
3140[s]	...	...	...	...	...	...	41	6658	6652	6655	3.72	3.72	2.4	75	1.63	3.00	-0.02	0.00
3184[s]	...	...	...	...	...	...	41	6263	6282	6272	3.84	3.83	2.1	59	2.45	2.71	-0.21	0.00
3202	109	22	38	30	49	23	34	6294	6266	6280	4.30	4.30	1.5	8	3.70	2.61	-0.08	-0.07±0.08
3220[e]	...	9	20	22	...	...	<1	6355	6331	6343	4.15	4.16	1.7	10	3.25	<0.97	-0.22	-0.36±0.06
3299	...	6	19	22	36	14	26	6510	6466	6488	4.12	4.13	1.8	8	2.98	2.63	-0.18	-0.31±0.05
3546[s]	...	...	...	...	...	...	28	6827	6905	6866	3.77	3.76	2.4	40	1.52	2.95	0.27	-0.22
3620[s]	...	...	...	...	...	...	45	6715	6692	6703	3.87	3.87	2.2	55	2.00	3.05	-0.03	-0.32
3775	91	27	30	22	44	18	100	6375	6352	6364	4.11	4.11	1.8	7	3.09	3.33	-0.15	-0.14±0.16
3857	94	14	24	23	37	9	<2	6806	6773	6789	4.11	4.11	1.9	19	2.59	<1.73	0.02	-0.02±0.12
3859[s]	...	...	...	...	...	...	62	6641	6639	6640	3.78	3.78	2.3	100	1.80	3.15	0.03	0.00
3954	116	29	37	33	81	35	22	6425	6410	6417	4.11	4.12	1.8	15	2.98	2.48	0.05	0.21±0.13
4012	196	30	43	41	65	34	<5	6252	6272	6262	4.17	4.17	1.6	11	3.30	<1.61	0.23	0.09±0.06
4079	...	10	22	23	35	10	21	6273	6287	6280	4.04	4.04	1.8	12	3.07	2.38	-0.38	-0.40±0.09
4130	151	27	38	32	80	47	9	6405	6407	6406	4.16	4.16	1.7	9	3.10	<1.99	0.17	0.19±0.13
4130[e]	...	23	36	34	...	...	8	...	...	...	...	...	...	...	...	...	...	...
4134[e]	...	12	24	18	...	...	16	6110	6152	6131	4.14	4.13	1.6	9	3.52	2.11	-0.35	-0.47±0.07
4150	85	15	25	22	38	17	4	6304	6315	6310	3.99	3.99	1.9	9	2.90	1.63	-0.38	-0.32±0.10
4158	96	18	27	29	51	21	43	6064	6100	6082	4.24	4.23	1.5	6	3.84	2.56	-0.28	-0.31±0.06
4251	107	22	37	35	58	28	11	6425	6429	6427	4.19	4.19	1.7	7	3.17	2.15	0.18	0.07±0.04
4251[e]	...	23	37	39	...	...	13	...	...	...	...	...	...	...	...	...	...	...
4298[e]	...	23	44	46	...	...	34	6263	6253	6258	4.26	4.26	1.5	6	3.56	2.56	0.09	0.05±0.06

TABLE 1—*Continued*

HR	Equivalent Widths (mÅ)							Effective Temperature (K)			log g		ξ^a	v sin i[a]	M_V	log ε(Li)	[Fe/H]	[Fe/H]
	Fe						Li	(β)	(b-y)	Mean	(β)	(b-y)					phot	spec
	6678	6703	6705	6726	6750	6752	6707											
4384[e]	...	16	25	26	...	...	<1	6453	6414	6433	4.20	4.21	1.7	8	3.24	<0.39	-0.08	-0.05±0.10
4399[b]	92	13	29	24	50	23	66	6730	6748	6739	3.98	3.97	2.1	13	2.24	3.25	0.17	0.06±0.06
4408	184	7	21	23	22	10	53	6675	6634	6654	3.88	3.88	2.2	32	2.12	3.14	-0.21	-0.25±0.11
4416[s]	...	...	...	...	...	...	30	6463	6462	6462	4.00	4.00	1.9	50	2.59	2.70	0.10	0.13
4431	95	14	23	21	48	16	48	6187	6205	6196	4.11	4.10	1.7	5	3.32	2.71	-0.29	-0.35±0.06
4479[se]	...	...	...	...	...	...	43	6869	6803	6836	4.07	4.08	2.0	50	2.48	3.10	-0.19	-0.17
4488	94	16	24	29	49	22	47	6176	6191	6184	4.20	4.19	1.6	5	3.60	2.69	-0.30	-0.27±0.07
4540	117	32	47	42	67	32	14	6187	6192	6190	4.20	4.20	1.6	6	3.49	2.12	0.13	0.10±0.07
4548[e]	...	24	36	34	...	...	45	6187	6178	6183	4.26	4.26	1.5	6	3.70	2.72	-0.04	-0.06±0.04
4600[e]	...	12	22	22	...	...	<1	6607	6548	6577	4.22	4.23	1.7	7	3.14	<1.36	-0.13	-0.15±0.05
4761	99	21	33	31	54	22	13	6041	6080	6060	4.08	4.08	1.7	5	3.39	1.99	-0.16	-0.24±0.08
4782[s]	...	...	...	...	...	...	34	6683	6653	6668	4.16	4.16	1.8	50	2.83	2.90	0.07	0.13
4821[sb]	...	...	...	...	...	...	15	6675	6697	6686	3.82	3.82	2.2	80	1.85	2.50	0.15	0.00
4856	113	22	34	37	57	26	<1	6132	6164	6148	3.90	3.89	2.0	12	2.74	<0.64	-0.10	-0.13±0.03
4981	98	15	25	26	45	17	88	6294	6297	6296	3.99	3.99	1.9	12	2.88	3.15	-0.27	-0.24±0.03
5011	126	36	51	48	73	38	81	6006	6030	6018	4.21	4.20	1.5	7	3.72	2.82	0.04	0.08±0.06
5048[sc]	...	...	...	...	...	...	15	6699	6645	6672	4.15	4.15	1.8	35	2.82	2.50	-0.07	-0.07±0.01
5083[s]	...	...	...	...	...	...	6	6798	6780	6789	3.95	3.95	2.1	60	2.14	2.20	0.03	-0.27
5098[sc]	...	...	...	...	...	...	<4	6633	6579	6606	4.23	4.24	1.7	15	3.12	<1.80	-0.02	0.23
5128[sc]	...	...	...	...	...	...	95	6699	6668	6684	4.10	4.10	1.9	40	2.65	3.50	0.04	0.08
5235[b]	133	42	53	51	76	43	<7	6176	6262	6219	4.01	3.99	1.8	11	2.86	<1.81	0.37	0.30±0.05
5257[sc]	...	...	...	...	...	...	20	6500	6504	6502	4.00	4.00	1.9	40	2.54	2.50	0.15	0.13
5258	111	29	46	33	53	25	18	6345	6351	6348	4.03	4.03	1.9	16	2.82	2.31	0.09	0.04±0.13
5304[b]	106	29	40	35	63	29	44	6220	6222	6221	4.11	4.11	1.7	10	3.21	2.65	0.02	-0.03±0.09
5317[b]	114	21	34	31	47	17	34	6425	6410	6417	4.04	4.04	1.9	26	2.78	2.67	0.01	-0.02±0.12
5322	128	47	51	48	77	43	18	6143	6161	6152	4.16	4.16	1.6	8	3.42	2.15	0.14	0.20±0.08
5338	88	17	27	26	58	24	<2	6121	6151	6136	4.00	4.00	1.8	13	3.08	<1.21	-0.17	-0.31±0.13
5363	116	9	30	28	49	20	56	6425	6416	6420	3.90	3.90	2.0	31	2.41	2.93	-0.09	-0.09±0.10
5404	106	25	35	29	55	25	18	6355	6321	6338	4.29	4.29	1.5	28	3.59	2.32	-0.05	-0.05±0.08
5426[sc]	...	...	...	...	...	...	59	6537	6528	6532	4.13	4.13	1.8	31	2.89	3.05	0.12	0.03
5434[s]	...	...	...	...	...	...	24	6827	6853	6840	3.98	3.98	2.1	55	2.17	2.80	0.19	0.08
5441	113	22	35	32	57	22	<2	6345	6348	6347	4.05	4.05	1.8	5	2.88	<1.30	0.11	-0.03±0.05
5445[c]	...	11	23	27	43	16	<1	6482	6444	6463	4.12	4.13	1.8	15	3.07	<1.06	-0.37	-0.27±0.03
5455	96	16	26	23	48	29	<3	6325	6302	6313	4.21	4.22	1.6	14	3.45	<1.50	-0.21	-0.19±0.11
5457[sc]	...	...	...	...	...	...	33	6304	6300	6302	4.16	4.16	1.7	15	3.24	2.60	0.09	0.18
5529	75	5	14	15	13	8	<3	6666	6598	6632	4.16	4.17	1.8	15	2.94	<1.67	-0.25	-0.51±0.10
5533	103	21	36	30	60	26	13	6510	6506	6508	4.17	4.17	1.7	15	3.00	2.30	0.17	0.09±0.07
5583	112	22	31	34	49	25	14	6355	6332	6344	4.25	4.25	1.6	6	3.45	2.19	0.06	-0.05±0.05
5612	121	24	39	36	51	30	44	6581	6563	6572	4.17	4.17	1.7	18	2.96	3.01	0.12	0.24±0.09

TABLE 1—*Continued*

HR	Equivalent Widths (mÅ) Fe 6678	6703	6705	6726	6750	6752	Li 6707	Effective Temperature (K) (β)	(b-y)	Mean	log g (β)	(b-y)	ξ^a	v sin i[a]	M_V	log ε(Li)	[Fe/H] phot	[Fe/H] spec
5691	111	20	34	35	58	25	8	6198	6198	6198	4.17	4.17	1.6	4	3.41	1.87	0.02	-0.10±0.02
5694	100	21	32	33	63	35	<3	6064	6091	6077	4.07	4.07	1.7	5	3.30	<1.28	-0.06	-0.15±0.11
5700[c]	...	16	26	31	...	...	<4	6365	6343	6354	4.12	4.13	1.7	21	3.15	<1.72	-0.22	-0.14±0.08
5716[s]	...	...	...	...	...	...	77	6875	6858	6867	4.05	4.05	2.0	70	2.36	3.50	0.06	0.08
5723[b]	84	11	21	21	44	16	69	6415	6396	6405	4.00	4.01	1.9	9	2.72	3.06	-0.10	-0.29±0.07
5803[c]	...	22	34	37	...	...	31	6415	6372	6393	4.29	4.29	1.5	7	3.52	2.66	-0.09	0.04±0.08
5921[c]	...	...	17	18	...	...	25	6699	6627	6663	4.13	4.14	1.8	11	2.86	2.77	-0.36	-0.19±0.06
5927	109	16	29	31	50	26	107	6491	6472	6481	4.09	4.09	1.8	6	2.83	3.46	0.05	0.04±0.05
5936[s]	...	...	...	...	...	...	59	6927	6889	6908	4.04	4.05	2.0	70	2.32	3.34	-0.05	-0.02
5954[scb]	...	...	...	...	...	...	<2	6284	6273	6278	4.14	4.14	1.7	15	3.23	1.40	-0.04	0.28
5986[b]	127	33	45	40	69	34	<7	6304	6313	6309	4.13	4.13	1.7	27	3.13	<1.86	0.16	0.20±0.06
6109[cb]	...	11	9	14	...	...	23	6999	6914	6956	4.30	4.32	1.7	19	3.06	2.93	-0.20	-0.17±0.25
6243[b]	104	20	33	31	55	26	<3	6405	6401	6403	3.89	3.89	2.1	9	2.39	<1.55	-0.01	0.00±0.04
6314[b]	96	15	27	29	50	26	73	6573	6580	6577	4.29	4.29	1.6	8	3.27	3.19	0.24	0.02±0.07
6375	...	12	32	32	71	18	25	6453	6424	6439	4.05	4.05	1.9	30	2.81	2.55	-0.13	-0.02±0.14
6394	127	21	29	28	51	18	96	6165	6192	6179	3.92	3.92	1.9	8	2.77	3.13	-0.11	-0.14±0.13
6400[e]	...	29	43	38	...	...	40	6121	6141	6131	4.12	4.12	1.7	8	3.33	2.57	0.11	0.01±0.06
6405[e]	...	17	24	26	...	...	35	6315	6304	6309	4.19	4.19	1.6	8	3.42	2.65	-0.34	-0.19±0.11
6409	115	24	42	36	62	32	<1	6444	6460	6452	4.05	4.05	1.9	7	2.74	<1.09	0.18	0.16±0.03
6409[e]	...	25	36	39	...	...	<2	...	...	...	...	...	...	...	...	...	...	...
6441	122	32	44	40	68	34	<3	6187	6248	6218	4.07	4.06	1.8	7	3.05	<1.41	0.32	0.12±0.04
6467	71	7	13	15	24	6	<5	6472	6447	6460	4.13	4.13	1.8	7	3.13	<1.84	-0.54	-0.55±0.10
6489	103	17	24	26	34	13	77	6385	6368	6377	4.00	4.01	1.9	13	2.77	3.11	-0.16	-0.20±0.12
6492[sc]	...	...	...	...	...	...	23	6895	6957	6926	3.98	3.97	2.1	35	2.08	2.85	0.26	-0.02
6496	117	22	41	36	63	31	<4	6304	6298	6301	4.10	4.10	1.7	10	3.10	<1.60	0.02	0.07±0.03
6541	100	16	25	26	47	19	<7	6220	6241	6231	3.97	3.97	1.9	8	2.89	<1.83	-0.27	-0.28±0.02
6710[sb]	...	...	...	...	...	...	12	6761	6703	6732	4.14	4.15	1.8	60	2.76	2.40	-0.09	-0.12
6761[eb]	...	29	37	35	...	...	18	5909	5956	5933	4.27	4.27	1.4	5	4.06	1.98	-0.11	-0.17±0.04
6836[cb]	...	15	26	32	52	21	36	6121	6133	6127	4.30	4.30	1.4	8	3.95	2.48	-0.24	-0.27±0.03
6987[sb]	...	...	...	...	...	...	<2	6699	6642	6670	4.05	4.06	1.9	60	2.57	<1.60	-0.17	-0.42
7034[e]	...	9	21	35	39	25	<6	6325	6305	6315	4.18	4.18	1.6	22	3.33	<1.83	-0.09	-0.24±0.17
7061[e]	...	15	28	34	51	25	<2	6395	6374	6384	4.04	4.05	1.8	15	2.88	<1.37	-0.18	-0.04±0.04
7126[e]	...	16	40	30	50	26	<0?	6555	6520	6537	4.20	4.20	1.7	15	3.10	<0.46	0.02	0.06±0.07
7163	100	15	31	29	53	28	64	6294	6292	6293	3.99	3.99	1.9	10	2.83	2.93	-0.12	-0.12±0.07
7172[c]	...	20	34	40	65	31	<5	6052	6095	6074	3.94	3.94	1.9	20	2.96	<1.61	-0.09	-0.07±0.06
7263[s]	...	...	...	...	...	...	15	6746	6675	6711	4.22	4.23	1.7	55	3.00	2.50	-0.14	0.08
7266[s]	...	...	...	...	...	...	22	6970	6937	6954	4.13	4.14	1.9	80	2.53	2.90	-0.01	0.03
7297[e]	...	20	27	31	...	...	<2	6263	6256	6259	4.17	4.17	1.6	10	3.41	<1.32	-0.23	-0.05±0.13
7322	93	18	19	27	41	16	<4	6315	6299	6307	4.17	4.17	1.7	6	3.34	<1.65	-0.24	-0.28±0.10

TABLE 1—*Continued*

HR	Equivalent Widths (mÅ) Fe 6678	6703	6705	6726	6750	6752	Li 6707	Effective Temperature (K) (β)	(b-y)	Mean	log g (β)	(b-y)	ξ[a]	v sin i[a]	M_V	log ε(Li)	[Fe/H] phot	[Fe/H] spec
7354	94	15	23	23	38	20	<7	6355	6333	6344	4.22	4.23	1.6	10	3.48	<1.90	-0.34	-0.29±0.08
7389[c]	...	15	38	39	62	28	49	6500	6497	6499	3.95	3.96	2.0	23	2.43	2.94	0.10	0.14±0.07
7438[s]	...	...	...	...	...	...	<5	6564	6507	6535	4.22	4.23	1.7	65	3.19	<1.90	-0.13	0.03
7451	96	14	26	30	51	25	54	6335	6310	6322	4.23	4.23	1.6	8	3.50	2.85	-0.25	-0.18±0.08
7496	97	17	29	22	52	22	25	6482	6457	6469	4.07	4.07	1.8	8	2.81	2.64	0.00	-0.05±0.08
7534	97	25	33	29	47	17	26	6375	6343	6359	4.22	4.22	1.6	8	3.38	2.55	-0.13	-0.09±0.12
7538[sc]	...	...	...	...	...	...	30	6472	6444	6458	4.01	4.01	1.9	18	2.73	2.72	-0.28	-0.32
7658	113	24	36	31	55	27	<1	6304	6302	6303	4.05	4.05	1.8	7	2.96	<1.07	0.00	0.00±0.06
7692[c]	...	...	27	30	...	20	21	6607	6571	6589	4.06	4.07	1.9	34	2.67	2.60	-0.04	-0.01±0.02
7697	92	13	24	27	42	22	5	6675	6620	6647	4.23	4.24	1.7	10	3.07	1.95	-0.02	-0.07±0.05
7727	106	27	38	35	62	29	<7	6241	6260	6251	4.05	4.05	1.8	13	2.98	<1.80	0.15	-0.04±0.07
7822[s]	...	...	...	...	...	...	43	6841	6815	6828	4.07	4.07	2.0	70	2.43	3.10	0.05	-0.22
7855	94	18	32	32	59	25	25	6041	6078	6059	4.12	4.12	1.6	10	3.50	2.30	-0.17	-0.25±0.11
7877[c]	...	4	13	16	19	8	27	6921	6851	6886	4.29	4.30	1.7	13	3.03	2.93	-0.09	-0.34±0.05
7907	114	35	51	42	61	27	42	6405	6370	6388	4.35	4.35	1.5	10	3.68	2.76	0.05	0.19±0.13
8031[c]	...	12	25	...	...	...	<3	6746	6676	6711	4.23	4.23	1.7	21	2.69	<1.82	-0.13	-0.01±0.03
8048[c]	...	...	23	25	...	...	82	6633	6601	6617	4.14	4.14	1.8	38	2.84	3.32	0.03	-0.12±0.02
8077	102	23	42	35	54	17	<4	6121	6140	6130	4.11	4.11	1.7	5	3.35	<1.41	-0.09	-0.20±0.15
8205	102	16	28	22	48	26	15	6555	6519	6537	4.21	4.22	1.7	16	3.13	2.39	0.02	-0.04±0.07
8245[s]	...	...	...	...	...	...	<3	6564	6499	6532	4.26	4.27	1.6	45	3.33	<1.70	-0.25	-0.22
8250	110	16	33	29	56	24	6	6294	6288	6291	4.08	4.08	1.8	8	3.04	1.80	0.00	-0.07±0.05
8315[scb]		...	...	...	...	...	51	6599	6560	6579	3.99	4.00	2.0	20	2.51	3.05	-0.48	-0.37
8354	70	8	9	14	25	10	<6	6315	6351	6333	4.11	4.10	1.7	6	3.30	<1.83	-0.68	-0.65±0.12
8391[s]	...	...	...	...	...	...	76	6472	6457	6465	3.84	3.84	2.1	50	2.24	3.20	-0.24	0.03
8447	101	18	32	35	59	27	29	6491	6452	6471	4.35	4.35	1.5	12	3.58	2.67	0.07	0.06±0.07
8457	105	22	36	34	50	19	11	6273	6271	6272	4.04	4.04	1.8	7	2.98	2.02	-0.05	-0.08±0.08
8462[s]	...	...	...	...	...	...	<2	6761	6712	6737	4.08	4.09	1.9	45	2.59	<1.50	-0.07	-0.27
8472	108	27	31	33	64	32	11	6263	6273	6268	3.96	3.96	1.9	10	2.74	2.03	0.03	0.04±0.11
8536	103	15	26	23	40	16	16	6187	6216	6202	3.90	3.89	2.0	7	2.71	2.20	-0.22	-0.31±0.07
8665	90	10	21	16	53	27	30	6165	6187	6176	4.17	4.17	1.6	8	3.55	2.47	-0.31	-0.37±0.16
8697[b]	96	15	22	23	45	17	<1	6121	6164	6142	4.05	4.04	1.8	4	3.24	<0.82	-0.31	-0.41±0.04
8805	87	16	27	24	37	9	<7	6616	6561	6589	4.21	4.22	1.7	10	3.09	<2.10	-0.08	-0.16±0.14
8825	82	11	22	27	48	24	<5	6315	6302	6308	4.14	4.14	1.7	14	3.27	<1.68	-0.27	-0.29±0.13
8848[sc]	...	...	...	...	...	...	76	6555	6526	6541	3.88	3.89	2.1	80	2.26	3.20	-0.23	-0.27
8853	112	30	44	50	64	35	62	6143	6146	6145	4.23	4.23	1.5	5	3.66	2.76	-0.07	0.01±0.12
8859[s]	...	...	...	...	...	...	20	6546	6500	6523	4.19	4.19	1.7	25	3.10	2.50	-0.08	-0.02
8955[s]	...	...	...	...	...	...	5	6220	6243	6232	3.84	3.83	2.1	40	2.44	1.60	-0.02	-0.17
8969	101	14	29	28	54	23	27	6110	6129	6119	4.19	4.18	1.6	7	3.62	2.33	-0.19	-0.30±0.07
9020[s]	...	...	...	...	...	...	49	6564	6526	6545	3.96	3.97	2.0	70	2.49	2.95	-0.24	-0.27
9059[b]	110	35	41	28	52	17	<1	6325	6330	6327	3.89	3.89	2.0	13	2.49	<0.72	-0.09	-0.01±0.17
9072[sb]	...	...	...	...	...	...	67	6581	6570	6576	3.70	3.71	2.4	40	1.69	3.20	-0.12	-0.27
9078	...	20	37	35	58	27	<3	6315	6300	6307	4.16	4.16	1.7	21	3.25	<1.48	0.00	-0.01±0.02

[a] Units of km s^{-1}.
[b] Stars labeled as single-lined spectroscopic binaries in the *Bright Star Catalogue* (Holfleitt 1982).
[c] McDonald CCD spectra.
[e] ESO spectra.
[s] Rapidly rotating star for which abundances were determined by fitting synthetic spectra. Li equivalent widths quoted are calculated from the synthetic fit.

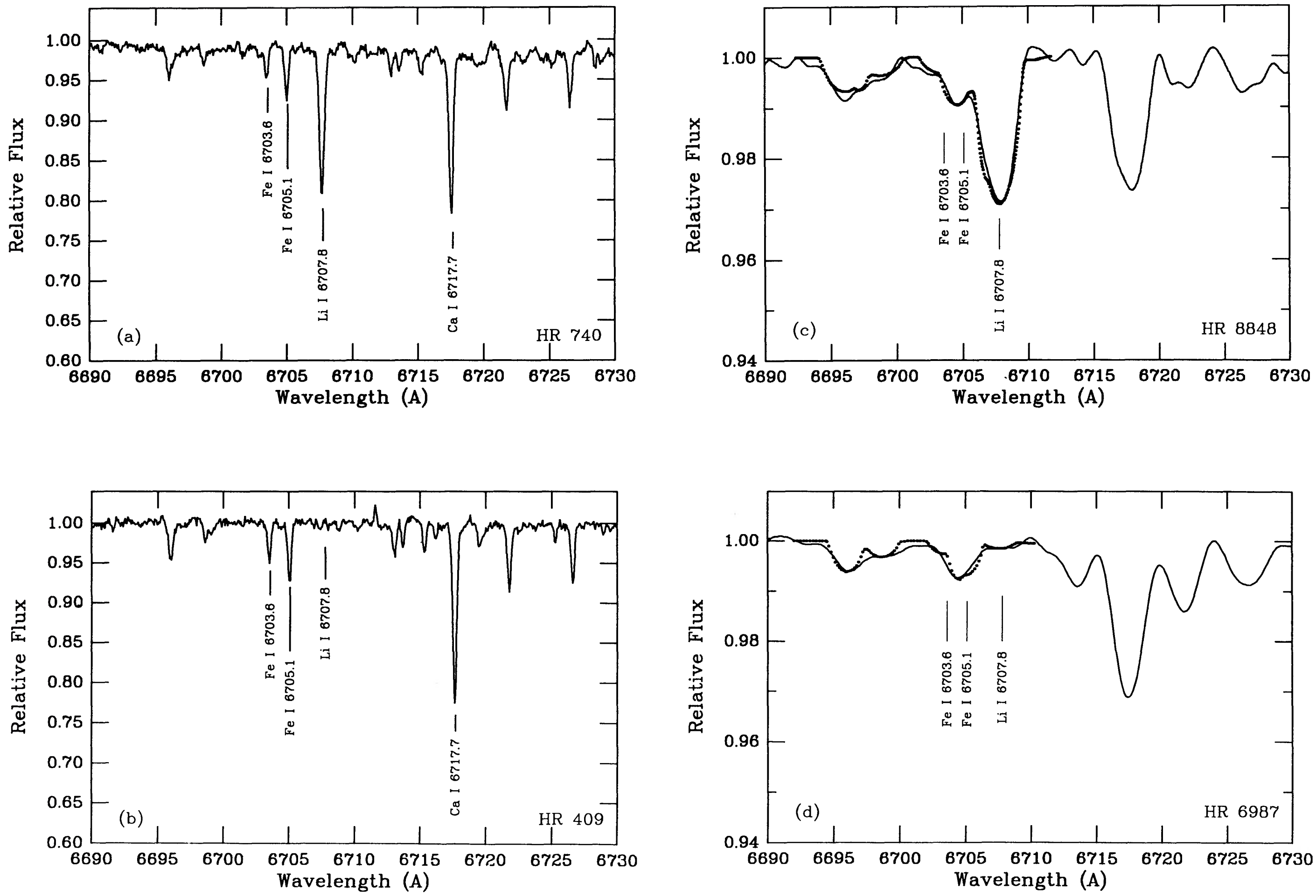

conceived as a time-saving device in the analysis of our large sample. In the above discussion, the ^{6}Li contribution to the Li feature is considered negligible. This assumption leads to an over estimation in the Li abundance of at most 0.05 dex when the abundances are derived from large equivalent widths.

b) *Rotational Velocities*

The solar spectrum obtained with each instrument-detector setup was broadened to various rotational velocities between 0 and 150 km s^{-1} by convolving it with the rotation profile of a spherical rigid body (Gray 1976). The FWHM of the Fe I line at 6678 Å and the Ca I line at 6717 Å was measured at each velocity. A relation between the FWHM and the rotational velocity was established and used to estimate the rotational velocities (v sin i) of the stars in our sample (see Table 1). For a few stars, spectra were obtained with both the Reticon and the CCD detectors and the calibrations gave consistent rotational velocities. A systematic error may be present because the calibration was obtained using the solar spectrum which is at the lower end of our temperature interval. This is, however, expected to be small because our temperature range is only 1000 K. Besides, the emphasis here is not on estimating the v sin i very accurately but on providing an independent check on the v sin i's listed in the BSC. In Figure 2*a*, the v sin i's determined through this process are compared with those listed in

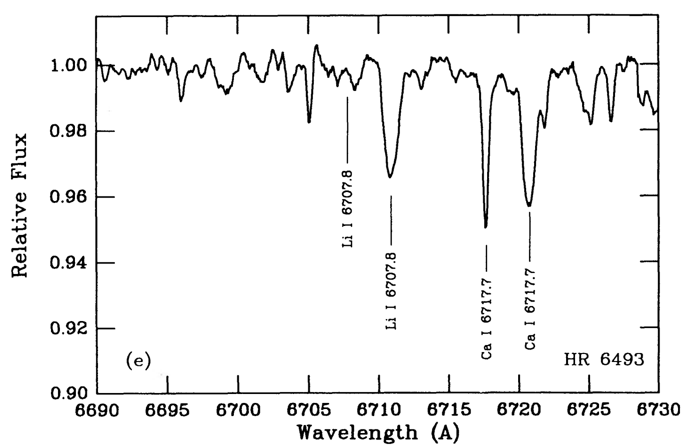

FIG. 1.—Five sample spectra are shown. HR 740 and HR 409 are both narrow-lined stars (v sin i = 7 and 6 km s^{-1}, respectively). The Li feature is strong in HR 740 and yields an abundance, log ϵ(Li) = 3.04. The Li feature is not detected in HR 409. An upper limit to the equivalent width was estimated at 3 mÅ yielding log ϵ(Li) < 1.30. HR 8848 and HR 6987 are both rapid rotators (v sin i = 80 and 60 km s^{-1}, respectively). The synthetic fits to their spectra are shown by dotted lines. The Li abundance is estimated to be 3.20 in HR 8848 and <1.60 in HR 6987. HR 6493 is a double-lined spectroscopic binary. The primary is a rapidly rotating F3 star in which the Li doublet is clearly seen. The slowly rotating companion is a F6 star which does not exhibit the Li doublet.

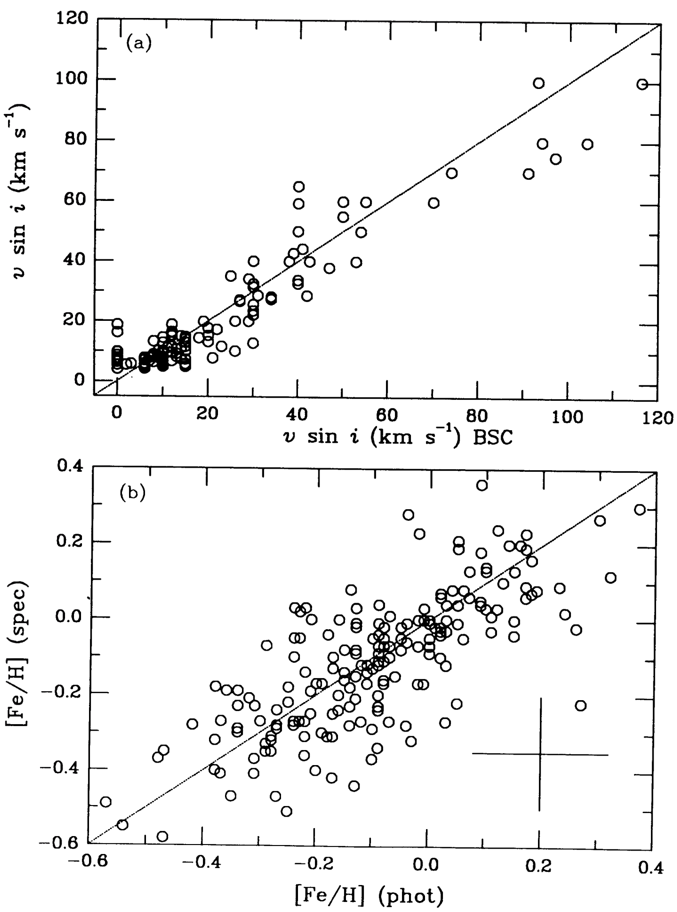

FIG. 2.—Comparing (*a*) projected rotational velocities, v sin i, measured from our spectra with those listed in the *Bright Star Catalogue* (Holfleitt 1982) and (*b*) spectroscopically measured [Fe/H] with photometric metallicities derived from the c_1 index. The dotted lines are 1:1 lines drawn for comparison. An estimate of the error in the Fe abundances in indicated in the lower right corner.

the BSC. The agreement is reasonable. Since our velocities have all been obtained from high-resolution spectra of similar quality, they should be internally more consistent.

Our measured velocities are good to ± 3 km s^{-1} at small velocities and reflect the accuracy of the FWHM measurement. At the high velocities, the v sin i estimate made by the above method was checked by fitting rotationally broadened synthetic spectra fitted to the stellar spectra and found to agree within ± 5 km s^{-1}.

c) *Model Atmospheres*

The solar model atmosphere obtained empirically by Holweger and Müller (1974, hereafter HM) was scaled to set up a grid of atmospheres at temperatures and gravities appropriate to our sample. The empirical model was preferred over the theoretical model atmospheres calculated by Kurucz (1979) mainly because it was felt that the empirical model was intrinsically more accurate than the theoretical models, which can only incorporate a certain finite number of lines in the opacity calculations. However, the empirical model must not be extrapolated too far from its effective temperature or metallicity in the scaling process. The stars in our sample range in effective temperature between 6000 and 7000 K, and the scaling process should be valid (Gray 1976). Further, as pointed out by Relyea and Kurucz (1978) and Steffen (1985), both the theoretical and empirical models have shortfalls at the temperatures of the F stars where convection is present but inefficient. Our interpretation of the abundances is based on the relative abundances between stars, and hence systematic inconsistencies should not be of major consequence.

Scaled solar models were obtained for effective temperatures between 5800 and 7000 K in 100 K intervals and gravities between 3.8 and 4.4 in steps of 0.2 dex. The scaling was done using a program written by Y. Chmielewski. The temperature of each layer was first scaled with effective temperature. The elements considered were H, He, C, N, O, Na, Mg, Al, Si, S, and Fe in its first and second ionization stage. The opacities considered were H^-, H, H_2^+, Rayleigh scattering by H and H_2, and bound-free absorption by C I, Mg I, Al I, Si I, and Fe I. Opacities were calculated, and the equation of hydrostatic equilibrium was integrated to obtain the scale model. Solar metallicities were assumed for all the models because the Li and Fe abundances showed only a small dependence on the metallicity of the model; the Li abundance changed by 0.01 dex and the Fe abundance changed by about 0.02 dex for changes in [Fe/H] of ± 0.3 dex in the metallicities of the models.

d) *Effective Temperatures*

Effective temperature, gravities, microturbulent velocities, and metallicities were obtained from Strömgren *uvby* Hβ indices. The indices for 162 stars were obtained from Olsen (1983). The rest were obtained from Hauck and Mermilliod (1980). Effective temperatures for F stars can be obtained either from the $b-y$ or the Hβ index. While the Hβ index is dependent only upon effective temperature, the $b-y$ index must be corrected for effects of interstellar reddening and line blanketing, and this was done using Crawford's (1975) empirical calibration of the Strömgren photometric system. Saxner and Hammarbäck's (1985, hereafter SH) empirical calibrations were then used to calculate effective temperatures from the corrected $(b-y)_0$ and the Hβ indices, and the mean of the two was adopted as the effective temperature of the star (Table 1). SH estimate that the error in the calibration is about ± 60 K. Errors in the effective temperature due to errors in the photometry are at most ± 80 K (Table 2). The effective temperatures obtained here are compared in Tables 3 and 4 with those obtained by Duncan (1981) and Boesgaard and Tripicco (1986*b*, hereafter BT) for stars which are in common with our sample. On the average, both the Duncan and BT temperatures are about 100 K lower than the temperature we obtained. Duncan's effective temperatures were derived partly from $R-I$ indices related to spectroscopically determined temperatures from Perrin *et al.* (1977) and partly from $B-V$ indices. Duncan reported a scatter of ± 70 K in the $R-I$ calibration, and Perrin *et al.* (1977) quoted an error of ± 160 K for their derived temperatures. We note that for three stars in common with BT, HR 4600, HR 7163, and HR 8205, the temperature differences are significantly different from the mean difference. BT used published Hβ indices (sources not cited) to obtain effective temperatures, and our adopted Hβ indices from Hauck and Mermilliod (1980) are 0.010 mag larger for HR 4600 and HR 7163 and 0.011 mag smaller for HR 8205 than the Hβ indices obtained by BT. These differences in the Hβ index lead to temperature differences of 100 K with the SH calibration. The adopted Hβ indices for the rest of the stars in common with BT are identical.

TABLE 2

RANDOM ERRORS CAUSED BY ERRORS IN THE PHOTOMETRY

Parameter	Error in Photometry	Error in Parameter
T_{eff}	Hβ: ± 0.0065 mag	± 80 K at 5800 K ± 45 K at 6900 K
	$b-y$: ± 0.0040 mag	∓ 25 K
$\log g$	Hβ: ± 0.0065 mag c_1: ± 0.0065 mag	∓ 0.002 dex at $\Delta \log g = -0.18$ ∓ 0.02 dex at $\Delta \log g = -0.18$
M_V	Hβ: ± 0.0065 mag c_1: ± 0.0065 mag	∓ 0.007 mag at $\Delta M_V = -0.52$ ∓ 0.07 mag at $\Delta M_V = -0.52$
[Fe/H]	Hβ: ± 0.0065 mag m_1: ± 0.0061 mag	∓ 0.01 dex at [Fe/H] $= -0.19$ ∓ 0.06 dex at [Fe/H] $= -0.19$
ξ	...	± 0.24 km s^{-1}

e) Gravities, Absolute Magnitudes, Metallicities, and Microturbulent Velocities

The Li abundance is very insensitive to changes in gravity. A change in the gravity of ± 0.3 dex changes the Li abundance by ∓ 0.01 dex for temperatures between 6000 and 7000 K. It is hence adequate to determine $\log g$ to within ± 0.3 for our analysis. Absolute magnitudes were first obtained from the δc_1 index using Crawford's (1975) calibration

$$\delta M_V = M_V - M_V(\mathrm{ZAMS}) = -(9 + 20\Delta\beta)\delta c_1 ,$$

where
$$\Delta\beta = 2.720 \text{ mag} - \beta .$$

Gravities were then obtained from Nissen and Gustafsson's (1978) calibration of Hejlesen's (1980) evolutionary tracks:

$$\log g\ (\mathrm{ZAMS, Population\ I}) = 5.30 - 1.375 \times 10^{-4} T_{eff} ,$$

$$\log g - \log g\ (\mathrm{ZAMS, Population\ I}) = 0.35\ \delta M_{bol} + 0.1\ [\mathrm{Fe/H}] .$$

Effective temperatures derived from both $(b-y)_0$ and Hβ indices were used to determine gravities and the mean value was adopted (Table 1). Errors in the photometry result in errors of about ± 0.02 dex in $\log g$ and ± 0.07 mag in absolute magnitude. Good agreement was found between the gravities obtained here and those obtained spectroscopically by Clegg, Lambert and Tomkin (1981) for the stars in common.

Metallicities were obtained from Nissen's (1981) calibration of the δm_1 index

$$[\mathrm{Fe/H}] = -[10.5 + 50(\beta - 2.626)]\delta m_1 + 0.16 ,$$

and they are listed in Table 1. Nissen estimated that the inter-

TABLE 3

COMPARISON OF TEMPERATURES, EQUIVALENT WIDTHS, AND ABUNDANCES WITH DUNCAN (1981)

HR Number	This Work				Duncan (1981)			
	T_{eff}	W_λ(mÅ)	log ϵ(Li)	[Fe/H]	T_{eff}	W_λ(mÅ)	log ϵ(Li)	[Fe/H]
33............	6071	28	2.35	−0.58	6208	50	2.56	0.09
143............	6279	<8	<1.97	−0.28	6194	...	...	−0.31
458............	6198	25	2.39	−0.03	6053	36	2.23	−0.06
544............	6288	<3	<1.50	0.00	6180	16	1.97	−0.03
781............	6423	28	2.59	−0.28	6266	21	2.18	−0.12
3202............	6280	34	2.61	−0.07	6194	<17	<1.98	−0.02
3775............	6364	100	3.33	−0.14	6252	108	3.14	−0.10
4012............	6262	<5	<1.61	0.09	5957	<20	<1.81	−0.05
4540............	6190	14	2.12	0.10	6138	<17	<1.95	0.21
5011............	6018	81	2.82	0.08	5943	121	2.97	0.04
5235............	6219	<7	<1.81	0.30	6095	<14	<1.81	0.40
5304............	6221	44	2.65	−0.03	6081	20	1.97	−0.03
5338............	6136	<2	<1.21	−0.31	6180	<16	<1.98	−0.10
5404............	6338	18	2.32	−0.05	6266	<25	<2.20	−0.17
5694............	6077	<3	<1.28	−0.15	6152	27	2.20	−0.04
5986............	6309	<7	<1.86	0.20	6281	<25	<2.30	0.04
7172............	6074	<5	<1.61	−0.07	6053	<12	<1.71	−0.03
7354............	6344	<7	<1.90	−0.29	6152	<28	<2.25	−0.45
7451............	6322	54	2.85	−0.18	6180	83	2.92	−0.19
7496............	6470	25	2.64	−0.05	6295	<16	<2.09	0.01
7534............	6359	26	2.55	−0.09	6237	35	2.42	−0.11
8665............	6176	30	2.47	−0.37	6012	21	1.94	−0.22
8697............	6142	<1	<0.82	−0.41	6026	47	2.39	−0.39
8969............	6119	27	2.33	−0.30	5970	23	1.95	−0.34

TABLE 4

COMPARISON OF TEMPERATURES, EQUIVALENT WIDTHS, AND ABUNDANCES WITH BOESGAARD AND TRIPICCO (1985b)

HR Number	This Work T_{eff}	This Work W_λ(Li + Fe) (mÅ)	This Work log ε(Li)	This Work [Fe/H]	Boesgaard and Tripicco (1986b) T_{eff}	Boesgaard and Tripicco (1986b) W_λ(Li + Fe) (mÅ)	Boesgaard and Tripicco (1986b) log ε(Li)	Boesgaard and Tripicco (1986b) [Fe/H]
3954	6417	23	2.48	0.21	6290	17	2.00	0.07
4150	6310	4	1.63	−0.32	6180	...	...	−0.33
4408	6654	55	3.14	−0.25	6575	64	2.95	−0.20
4600[a]	6578	< 3	< 1.36	−0.15	6390	< 4	< 1.28	−0.21
5445	6463	< 3	< 1.06	−0.27	6350	< 5	< 1.15	−0.11
5455	6313	< 5	< 1.50	−0.19	6170	< 6	< 1.38	−0.22
5529	6623	< 5	< 1.67	−0.51	6565	< 1	< 1.06	−0.39
5533	6508	16	2.30	0.09	6380	10	1.78	0.08
6467	6460	< 6	< 1.84	−0.55	6340	< 3	< 1.20	−0.41
6489	6377	79	3.11	−0.20	6225	93	2.93	−0.17
6541	6231	< 10	< 1.83	−0.28	6105	< 6	< 1.36	−0.22
7163[a]	6293	68	2.93	−0.12	6075	74	2.64	−0.19
7322	6307	< 6	< 1.65	−0.28	6190	< 4	< 1.02	−0.28
7697	6647	5	1.95	−0.07	6575	...	...	0.11
7727	6251	< 10	< 1.80	−0.04	6125	< 8	< 1.34	0.00
8205[a]	6537	18	2.39	−0.05	6545	23	< 2.38	0.17
8354	6332	< 7	< 1.83	−0.65	6190	< 3	1.65	−0.59
8805	6589	< 9	< 2.10	−0.16	6500	< 3	< 0.90	−0.07
8825	6308	< 7	< 1.68	−0.29	6190	< 2	< 1.15	−0.27

[a] Difference in effective temperature is due to the adopted Hβ index (see text in § IIId).

nal accuracy of the calibration was ±0.08. Errors in metallicity due to photometric errors are at most ±0.09, leading to a combined error of ±0.12 dex.

Finally, microturbulent velocities were obtained using Nissen's (1981) calibration

$$\xi_t = 3.2 \times 10^{-4}(T_{eff} - 6390) - 1.3(\log g - 4.16) + 1.7 ,$$

and they were found to range between 1.0 and 2.0 km s^{-1} (Table 1). An average value of 1.5 km s^{-1} was chosen for our analysis. Errors in the microturbulent velocity due to photometric errors are about ±0.24 km s^{-1}. Errors in the calibration are reported to be ±0.2 km s^{-1} (Nissen 1981), leading to a combined error of ±0.32 km s^{-1}.

Table 2 provides a summary of the errors in the effective temperature, gravity, absolute magnitude, photometric metallicity, and microturbulent velocity due to random errors in the photometry as listed in Olsen (1983). The errors in the compilation by Hauck and Mermilliod (1980) may be somewhat larger. However, these data were used for only 27 stars in our sample.

f) gf-Values

Equivalent widths of the Fe I lines present in our spectra were measued from the Photometric Atlas of the Solar Spectrum (Delboille, Roland, and Neven 1973). "Solar gf-values" were computed (Table 5) using the HM solar model and taking the solar Fe abundance log $\epsilon(Fe)_\odot = 7.67$. "Kurucz gf-values" were also computed using an interpolated Kurucz solar atmosphere with $T_{eff} = 5770$ K. The "Kurucz gf-values" are around 0.16 dex smaller than the "solar gf-values." The gf-values and wavelengths of the Li I resonance doublet are taken from Andersen, Gustafsson, and Lambert (1984). The Li gf-values are based on a radiative lifetime measurement made by Gaupp, Kuske, and Avda (1982).

g) Effects of Rapid Rotation on the Strömgren Colors

Rapid rotation changes the Strömgren colors of a star by changing its internal structure. The centrifugal force caused by rotation opposes gravity and causes the star to expand. The interior temperature drops, and less themonuclear energy is generated. The net result is a decrease in both the temperature and luminosity of the star. From Collins and Sonneborn (1977), we estimate that the effective temperature will decrease by about 100 K and the absolute magnitude will increase by 0.15 mag for the fastest rotators in our sample. This effect is much smaller for smaller rotational velocities.

We now consider the effects of rapid rotation if only the convective envelope of the star is affected by it. Böhm-Vitense (1981) suggested that there may be two separate branches in

TABLE 5

LINE DATA

Species	Wavelength (Å)	Equivalent Width (mÅ)	Excitation Potential (eV)	log gf
Fe I	6677.99	140	2.76	−1.33
Al I[a]	6696.03	33	3.14	−1.61
Fe I[a]	6696.32	16	4.83	−1.65
Al I[a]	6698.67	21	3.14	−1.87
Fe I[a]	6696.14	7	4.59	−2.27
Fe I[a]	6703.58	34	2.76	−3.15
Fe I[a]	6705.11	46	4.61	−1.15
Fe I[a]	6707.45	5	4.61	−5.30
Fe I[a]	6710.32	12	1.48	−4.99
Fe I[a]	6713.04	24	4.61	−1.61
Fe I[a]	6713.21	7	4.14	−2.69
Fe I[a]	6713.75	23	4.79	−1.48
Fe I	6726.67	49	4.61	−1.13
Fe I	6750.16	75	2.42	−2.66
Fe I	6752.72	38	4.64	−1.31

[a] These lines were used to obtain synthetic fits to broad-lined stars.

the T_{eff} versus $B-V$ relation between $B-V$ of 0.25 and 0.45 with the upper branch, populated by slow rotators, about 300–500 K higher than the lower branch, which is populated by more rapid rotators. In this $B-V$ range, SH have only rapid rotators in their sample, and their relation coincides with the lower branch in the Böhm-Vitense calibration. If a similar branching exists in the T_{eff} versus $(b-y)_0$ and Hβ relations, we are underestimating the temperatures and hence the Li abundances in our slow rotators by 0.3–0.5 dex.

h) Abundances

In the narrow-lined, slowly rotating stars, Li and Fe abundances were determined from the measured equivalent widths using the program LINES (Sneden 1973) (see Table 1). Identical Fe abundances were obtained through the entire temperature range of our sample when "solar *gf*-values" were used with scaled solar model atmospheres and "Kurucz *gf*-values" were used with Kurucz model atmospheres. When the same absolute Li I *gf*-values were used, Kurucz atmospheres yielded Li abundances about 0.15 dex lower than the scaled solar models. Since the absolute *gf*-values were used to determine the Li abundance and Li is severely depleted in the Sun, absolute Li abundances log ϵ(Li) are given on the usual scale where log ϵ(H) = 12.0. "Solar *gf*-values" have been used to determine Fe abundances, and hence, we give Fe abundances as $[\mathrm{Fe/H}] = \log\,(\mathrm{Fe/H})_{\mathrm{star}} - \log\,(\mathrm{Fe/H})_{\odot}$. The uncertainty in [Fe/H] corresponds to the internal error from the five or six measured Fe I lines. Rotationally broadened synthetic spectra were fitted to rapidly rotating, broad-lined stars. Both the abundance and the rotational velocity were adjusted until a good fit was obtained. Stars for which abundances were determined in this way are denoted with superscript "s" in Table 1, and the equivalent widths listed for the Li feature are derived from the synthetic fit. Sample spectra along with synthetic spectrum fits are shown in Figure 1.

For narrow-lined stars, the minimum uncertainty in the abundance is that resulting from the lines' equivalent widths (W_λ). This leads to Li abundance errors between ± 0.02 dex at large equivalent widths (100 mÅ) and ± 0.07 dex at small equivalent widths (10 mÅ). Errors in [Fe/H] due to equivalent width uncertainties range between ± 0.04 and ± 0.07 dex. In rapidly rotating stars, a change in the abundance of ± 0.1 dex noticeably worsened the fit of the synthetic spectrum and is probably a good reflection of the error in the abundance. Abundance uncertainties arising from errors in the atmospheric parameters are as follows:

$$\Delta T_{\mathrm{eff}}(\mathrm{K}) = \pm 80 \qquad \Delta \log \epsilon(\mathrm{Li}) = \pm 0.08$$
$$\Delta[\mathrm{Fe/H}] = \pm 0.07\,,$$
$$\Delta \log g(\mathrm{cm\ s^{-2}}) = \pm 0.2 \quad \Delta \log \epsilon(\mathrm{Li}) = \mp 0.00$$
$$\Delta[\mathrm{Fe/H}] = \mp 0.01\,,$$
$$\Delta \xi_{\mathrm{mic}}(\mathrm{km\ s^{-1}}) = \pm 0.5 \quad \Delta \log \epsilon(\mathrm{Li}) = \mp 0.02$$
$$\Delta[\mathrm{Fe/H}] = \mp 0.13\,.$$

Since the Li abundance is not greatly affected by the microturbulence, an average value of 1.5 km s^{-1} was selected for this analysis. However, the largest error in [Fe/H] is caused by the uncertainty in the microturbulence, and this could have been somewhat reduced by adopting the appropriate microturbulence for each star. If the uncertainties arising from W_λ, T_{eff}, g, and ξ_{mic} are added quadratically, we find Δ log ϵ(Li) = ± 0.08 to ± 0.11, depending upon the error in W_λ and Δ [Fe/H] = ± 0.15 to ± 0.16. Within these errors, there is good agreement between the spectroscopically determined [Fe/H] and photometrically determined metallicities (Fig. 2b).

Equivalent widths and abundances obtained here are compared with those from Duncan (1981) (Table 3) and BT (Table 4). The BT data are Reticon spectra of quality comparable to ours. Our Li equivalent widths in Table 4 include the Fe I blend so that they may be compared with the published values of BT. While the Fe abundances agree well within the errors, there are larger differences in the Li abundances. For the five stars with firm measurements of the 6707.8 Å feature, the mean difference in the Li abundance is 0.33 ± 0.06 dex. If equivalent width differences are allowed for the five stars, the mean difference is 0.30 ± 0.02 dex. The use of Kurucz models and a systematic 100 K lower temperature results in BT having a lower Li abundance by 0.25 dex. These systematic differences account for most of the 0.30 dex difference.

Duncan's (1981) observations were obtained using a wobble block to alternate between the line and continuum and photomultiplier tubes were used to record the "spectrum." Metallicities listed in Duncan's study come from a variety of sources including *uvby* and *UBV* photometry and spectroscopically determined [Fe/H] from Perrin *et al.* (1977). The differences in T_{eff} and model atmospheres leads to systematic differences in Li abundances similar to the differences noted above with BT. More importantly, Table 3 shows that there are sometimes large discrepancies between the equivalent widths of the Li I doublet measured by us and by Duncan. For example, we estimate the equivalent width of the Li I feature in HR 8697 to be less than 1 mÅ from our study, while Duncan reported it as 47 mÅ. We have two spectra of this star and the measurements are consistent. Such large discrepancies may be attributed directly to the larger observational errors in the technique used by Duncan.

IV. RESULTS

The solar system abundance of Li is 3.31 as derived from the Li content of meteorites with a normalization to hydrogen through spectroscopically determined solar abundances of selected metals (Anders and Grevesse 1989). Early observations of some T Tauri stars (Hunger 1957; Bonsack and Greenstein 1960) and early F stars in clusters (Herbig 1965; Wallerstein, Herbig, and Conti 1965) yielded a Li abundance around the meteoritic value, and this has since been used as the initial abundance of Population I stars. As noted previously, for a measured equivalent width, the calculated Li abundance depends primarily upon the choice of the model atmosphere and the effective temperature estimated for the star. The initial Li abundance of Population I stars is best estimated from young stars which have not undergone any Li depletion on the main sequence and from warmer F stars which are least likely to have undergone significant Li depletion during the pre–main-sequence phase (Bodenheimer 1965; D'Antona and Mazzitelli 1984). BLS obtain a Li abundance of 3.19 ± 0.04 from rapidly rotating stars in the young α Per cluster using an analysis similar to the one used here. This value is consistent with the value of 3.01 ± 0.15 adopted by BT when allowances are made for the 100 K difference between their temperature calibration and ours and their choice of Kurucz model atmospheres. We hence adopt the Li abundance of 3.20 as the *cosmic* value in the discussion that follows.

a) *Trends with Effective Temperature*

In Figure 3*a*, Li abundances are plotted against effective temperature with open circles for stars with measured Li abundances and filled triangles for stars with estimated upper limits. Although there is a large abundance range in each group, for convenience we will refer to these two groups as Li-measured and Li-depleted, respectively. The Li abundance varies by over a factor of 100 through the entire temperature range. The upper envelope of the Li abundances shows a gradual decrease in the Li abundance toward lower effective temperatures. At 7000 K, the maximum Li abundance is around 3.5, and this decreases to 2.5 by 6000 K. The lower envelope of the measured abundances does not show any trend with temperature; i.e., stars with an abundance of 2.0, a depletion of over a factor of 30 from the *cosmic* value, are found at all temperatures. The Li-depleted stars appear scattered through the entire temperature range. Recall that a constant measurable equivalent width limit, set by the spectrum quality, leads to larger abundances at higher temperatures, and hence an increase in the upper limits with temperature is not surprising. Our sample covers the effective temperature range 6000–7000 K, which includes the small temperature interval in which the Li "dip" was observed in the Hyades (Boesgaard and Tripicco 1986*a*). Li abundances at the *cosmic* value are seen at 6600 K, the center of the Li "dip" in the Hyades, and stars with large Li depletions are scattered through the entire temperature range; the "dip" is not obvious in Figure 3*a*. In Figure 3*b*, [Fe/H] is plotted against effective temperature. The Fe abundances do not show any trend with effective temperature. The mean [Fe/H] is around -0.2 with a range of ± 0.5 dex around the mean. Li depletion does not correlate with metallicity (Fig. 4). The entire range of Li abundances is seen in stars between metallicities of 0.4 to -0.4. The somewhat smaller spread in Li below -0.4 may be related to the sparsity of stars in our sample in this metallicity range.

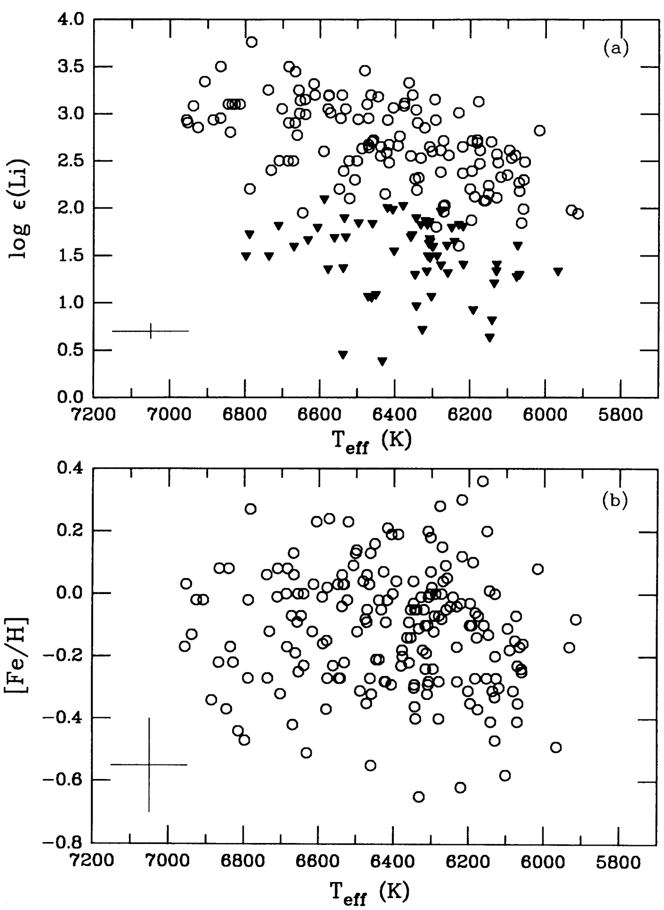

FIG. 3.—(*a*) Li abundances and (*b*) [Fe/H] vs. effective temperature. Open circles represent measured abundances and filled triangles represent upper limits. An estimate of the error in the abundance and the effective temperature is shown in the lower left corner.

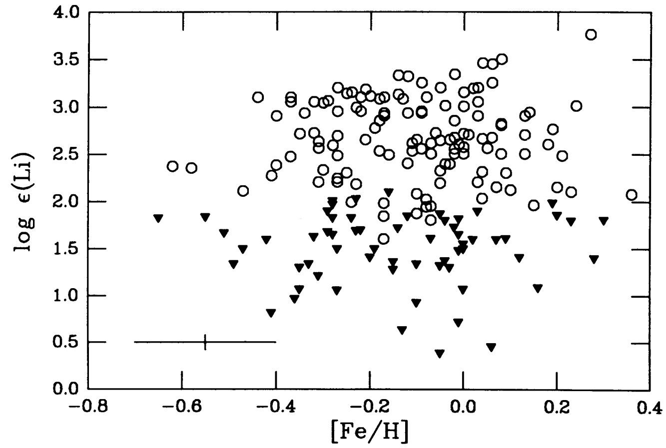

FIG. 4.—Li abundances vs. [Fe/H]. Open circles represent measured Li abundances, and filled triangles represent estimated upper limits to the Li abundances. An estimate of the errors in both abundances is shown in the lower left corner.

b) *Trends with v* sin *i*

In Figure 5*a*, Li abundances are plotted against $v \sin i$ with the symbols having the same meaning as before. Notice the concentration of Li-depleted stars at small $v \sin i$ values and the sparseness of these at large $v \sin i$'s; 42% of stars with $v \sin i < 30$ km s^{-1} have lithium abundances of less than 2.0 compared to 17% of those with $v \sin i > 30$ km s^{-1}. Note that there is no similar correlation between [Fe/H] and $v \sin i$ (Fig. 5*b*); [Fe/H] between 0.2 and -0.4, which covers almost the entire range of metallicities in our sample, are found at all rotational velocities. Although highly Li depleted stars are sparse at large $v \sin i$'s, the range among the Li-measured stars exceeds 1.0 dex even in the fastest rotators.

The entire sample was divided into six bins according to Li abundance and $v \sin i$ as shown by the dotted lines in Figure 5*a*. The bins were defined as follows:

bin A: $\log \epsilon(\text{Li}) \geq 2.0$ and $v \sin i \leq 20$ km s^{-1},
bin B: $\log \epsilon(\text{Li}) \geq 2.0$ and $20 < v \sin i \leq 50$ km s^{-1},
bin C: $\log \epsilon(\text{Li}) \geq 2.0$ and $v \sin i > 50$ km s^{-1},
bin D: $\log \epsilon(\text{Li}) < 2.0$ and $v \sin i \leq 20$ km s^{-1},
bin E: $\log \epsilon(\text{Li}) < 2.0$ and $20 < v \sin i \leq 50$ km s^{-1},
bin F: $\log \epsilon(\text{Li}) < 2.0$ and $v \sin i > 50$ km s^{-1}.

To examine variations in Li and $v \sin i$ with mass in stars which have evolved off the main sequence, the stars in the various bins are plotted on the H-R diagram along with the zero-age main sequence (ZAMS) taken from VandenBerg and Bridges (1984, hereafter VB) and evolutionary tracks for [Fe/H] = 0.0 taken from VandenBerg (1985) (Fig. 6). Progressively larger symbol sizes are used to represent increasing values of $v \sin i$. The VB ZAMS is displaced about 0.23 mag below the Craw-

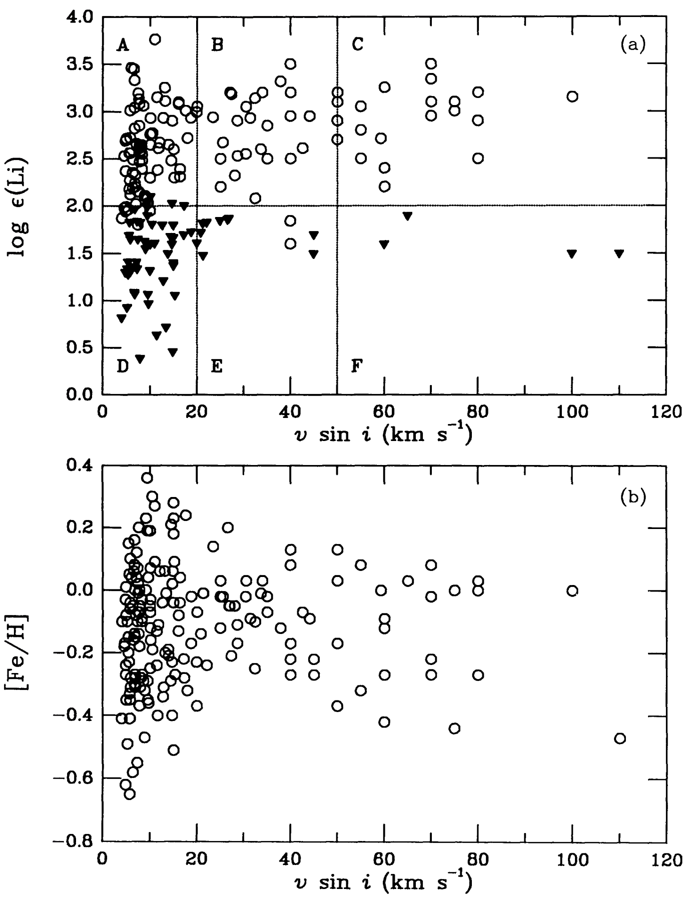

FIG. 5.—(*a*) Li abundances vs. $v \sin i$. Open circles represent measured Li abundances and filled triangles represent estimated upper limits. Dotted lines show the division of the sample into six bins, A–F. (*b*) [Fe/H] vs. $v \sin i$.

ford (1975) ZAMS. In accordance with VB's suggestion, both the ZAMS and the tracks have been shifted to cooler temperatures by 100 K. The Sun, with $M_V = 4.83$ and $T_{\rm eff} = 5770$ K, then falls reassuringly close to the intersection of a 1.0 $M_\odot$ track and a 5.0 Gyr isochrone, and the ZAMS coincides reasonably with the Crawford (1975) ZAMS. For convenience, the mass of the star is sometimes used to define its position in the H-R diagram and, unless explicitly mentioned otherwise, it refers to the mass as derived from these [Fe/H] = 0.0 evolutionary tracks. The stars in our sample have masses between 1.0 and 1.85 $M_\odot$ and ages between 1.25 and 8 billion years (as noted from isochrones; VandenBerg 1985).

We observe that the stars in bins A, B, and C, which are the Li-measured stars ordered in increasing $v \sin i$, are separated in the H-R diagram with the fastest rotators also being the most massive (Fig. 5). This reveals, as did the classic study by Kraft (1967), the slowing down of the lower mass stars due to the deepening convective envelope. Although there is an overlap between the bins, the mean mass of the fastest rotators, bin C, is larger than that of the intermediate rotators, bin B. The slowly rotating Li-measured stars contained in bin A are the least massive stars, though a few of these are scattered at masses of around 1.7 $M_\odot$. If rotation changes the temperature and luminosity of the entire star (see § III*g*), the masses of the most rapid rotators have been underestimated, and the overlap between bins B and C is actually larger. However, for a star rotating at 100 km s^{-1}, the predicted decrease in the effective temperature is probably less than 100 K and that in luminosity is about 0.15 mag (Collins and Sonneborn 1977), leading to a decrease in mass of at most 0.1 $M_\odot$. Some measure of overlap between the bins is inevitable because the projected rotational velocity, $v \sin i$, is measured and not v itself; the more massive stars in bin B may be rapid rotators seen at small inclinations. For a star rotating at 100 km s^{-1} to be observed rotating at less than 20 km s^{-1}, the inclination angle must be less than 12°. The probability that all the slowly rotating stars at higher masses are seen at small inclinations is hence small and some overlap must be intrinsic, i.e., there is a velocity distribution at each mass. The mean Li abundance of the 75 members in bin A is 2.63 ± 0.4, that of the 31 members in bin B is log ϵ(Li) $= 2.85 \pm 0.35$, and that of the 17 members in bin C is log ϵ(Li) $= 2.92 \pm 0.35$. The mean abundance in bin A will be higher if the branching in the $B-V$–$T_{\rm eff}$ relation discussed earlier is real, and the effective temperatures of the slow rotators have been underestimated. The mean Li abundance of the slow rotators will be much lower if we include the Li-depleted stars of bin D in this group. The reasons for not doing this will soon become apparent.

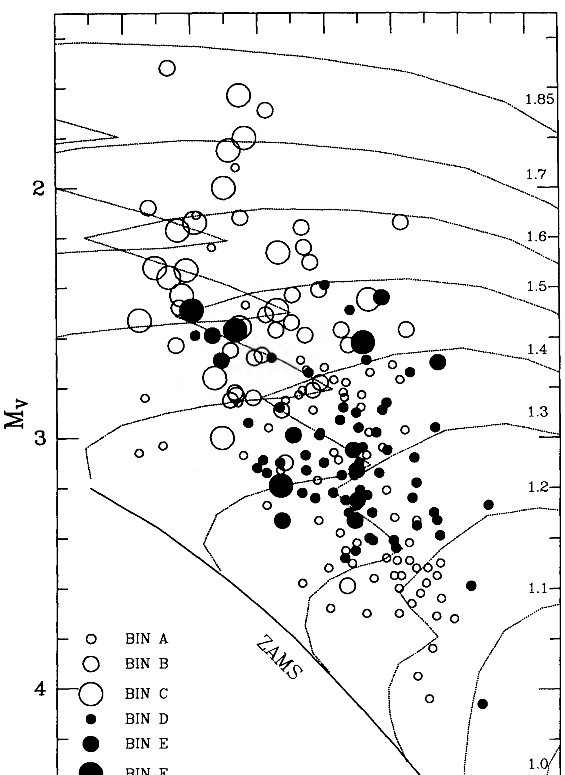

FIG. 6.—The entire sample is plotted on the H-R diagram. Stars have been grouped into six bins (see text and Fig. 5 for definitions of the bins) according to Li abundance and $v \sin i$. The size of the circle increases with $v \sin i$ (see key). Open circles represent stars with measured Li abundances and filled circles represent stars with estimated Li upper limits. The ZAMS and evolutionary tracks (*dotted lines*) are for [Fe/H] = 0.0 and are taken from VandenBerg and Bridges (1984) and VandenBerg (1985), respectively. Each evolutionary track is labeled in solar masses on the right-hand side of the figure.

c) Hyades Dip–like Stars

When the positions of bins A and D on the H-R diagram are compared (Fig. 6), we find that the slowly rotating Li-measured stars, bin A, appear to fall in two clumps in the H-R diagram, a higher mass clump around 1.4 $M_\odot$ and a lower mass clump around 1.2 $M_\odot$. The higher mass clump (defined here as those having $M_V < 3.25$ mag) has 40 members and a mean Li abundance log ϵ(Li) = 2.73 ± 0.5, while the low-mass clump ($M_V >$ 3.25 mag) has 35 members and a mean Li abundance, log ϵ(Li) = 2.51 ± 0.2. The Li-depleted slow rotators, bin D, appear to be concentrated in the gap between the two clumps which form bin A. Two observations lead us to believe that these are older, field counterparts of the Li-dip stars first seen in the Hyades (Boesgaard and Tripicco 1986*a*). First, the Li depleted stars are seen in the same mass range as the Hyades "dip" stars. They appear to have evolved from main-sequence effective temperatures between 6500 and 6800 K, the same temperature interval in which low Li abundances are observed in the Hyades. Second, the lower mass boundary of bin D is sharp. If the onset of highly Li depleted stars was merely an extension of the trend of increasing Li depletion toward lower masses (bin B has a lower mean Li abundance than bin C, etc.), such large Li depletions should continue to be seen at masses less than 1.2 $M_\odot$, where the convective zone is even deeper. Our sample includes a fair number of stars which have evolved from main-sequence effective temperatures around 6200 K, and such large depletions are not seen among them. Most of the Li-depleted stars of bin E are also in the midst of this Li-depleted clump along with one rapid rotator from bin F.

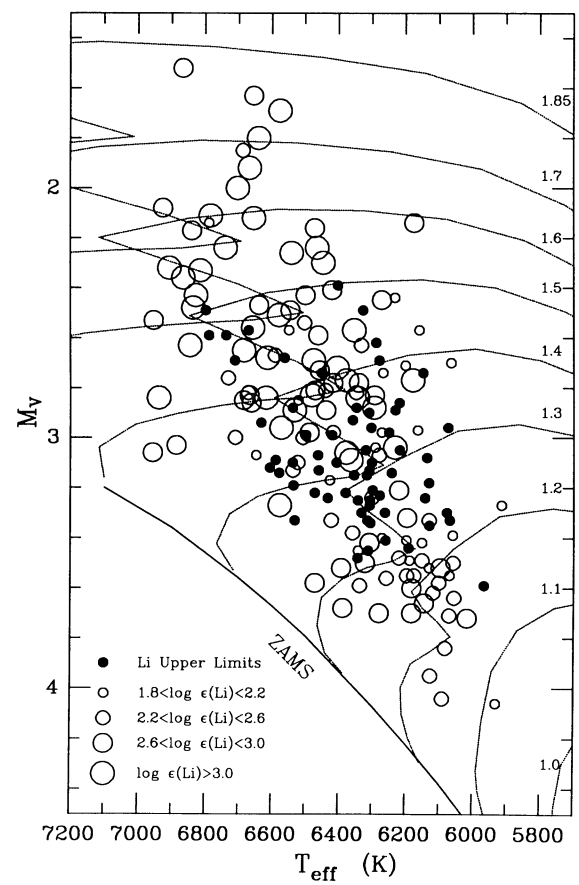

FIG. 7.—The entire sample plotted on the H-R diagram. The size of the open circle represents the Li abundance (see key), and the filled circle represents an upper limit. The ZAMS and evolutionary tracks are for [Fe/H] = 0.0 and are taken from VandenBerg and Bridges (1984) and VandenBerg (1985), respectively. Each evolutionary track is labeled in solar masses on the right-hand side of the figure.

The entire sample is plotted on the H-R diagram, with the symbol size now indicating the Li abundance (Fig. 7). It is clear that as we move across the H-R diagram from higher masses, the Li abundance drops in the region identified as that of the "dip" and rises again in lower mass stars. The Li-depleted stars are not as tightly clumped as one would expect from the Hyades observations. A few Li-depleted stars of all $v \sin i$'s are found at higher masses, and some stars with abundances between 2.6 and 3.0 are seen in the "dip" region. Apart from errors in $T_{\rm eff}$ and M_V that result from errors in photometry and calibrations, the evolutionary part of the stars in the H-R diagram probably adds to the smearing of the Li "dip." Tracks 1.2 $M_\odot$ and above show a blueward hook caused by rapid contraction after core hydrogen exhaustion and terminated by the onset of hydrogen shell burning. The end of this hook leaves the star about 0.4 mag brighter than before and places it along with stars of a higher mass which have not yet undergone the "hook" phase. The star does not live in the hook for a long time. According to VandenBerg (1985), a 1.3 $M_\odot$ star spends about 2% of the entire time spent in the track illustrated in Figure 7 in the blueward hook phase and about 16% of its time beyond the hook. However, just above the hook the 1.3 $M_\odot$ track almost coincides with the 1.4 $M_\odot$ track and higher mass tracks intersect each other, making it difficult to estimate the mass of the star. In this context, it is perhaps relevant to point out that the smearing is more pronounced at the high-mass end of the Li-depleted clump, where this hook phase is more prominent.

Similar to our observations (Fig. 3), BT's earlier study of Li abundances in F stars found that Li-depleted stars were seen at all effective temperatures. They suggested that a combination of age and rotation may be responsible for the large Li depletion seen in some stars. If we plot data from BT and Boesgaard and Tripicco (1987) which are not in common with our sample on the H-R diagram (Fig. 8), it once again becomes apparent that although the Li-depleted stars are somewhat spread in $T_{\rm eff}$, they are clumped in mass. A cluster of Li-depleted stars is seen around the 1.4 $M_\odot$ track between the ZAMS and the blueward hook phase, though the intrusion of a few stars with higher Li abundances persists. It is clear that the Li-depleted stars are not simply older stars as suggested by BT. Our sample contains several older, less massive stars, and Li-depleted stars are not abundant among them. Boesgaard (1987*b*) pointed out that in the Hyades, the decrease in the Li abundance between 6300 and 6600 K coincided with a sharp increase in rotational velocity in these stars, suggesting that some form of rotational mixing may be responsible for the "dip." In our data, the sharp drop in rotational velocity is seen between bins B and A (Fig. 6) which occurs at a mass of around 1.4 $M_\odot$ and is far removed from the rise in Li from the "dip" region referred to above, which occurs at a mass of around 1.3 $M_\odot$. The "dip" stars in the field are themselves rotating slowly and are flanked on both the high- and low-mass sides by slowly rotating stars with Li abundances as large as 3.0.

The 57 Li-depleted stars in our sample span the entire metallicity range between −0.6 and 0.4, and this may be one of the factors causing the smearing of the Li-depleted clump in the

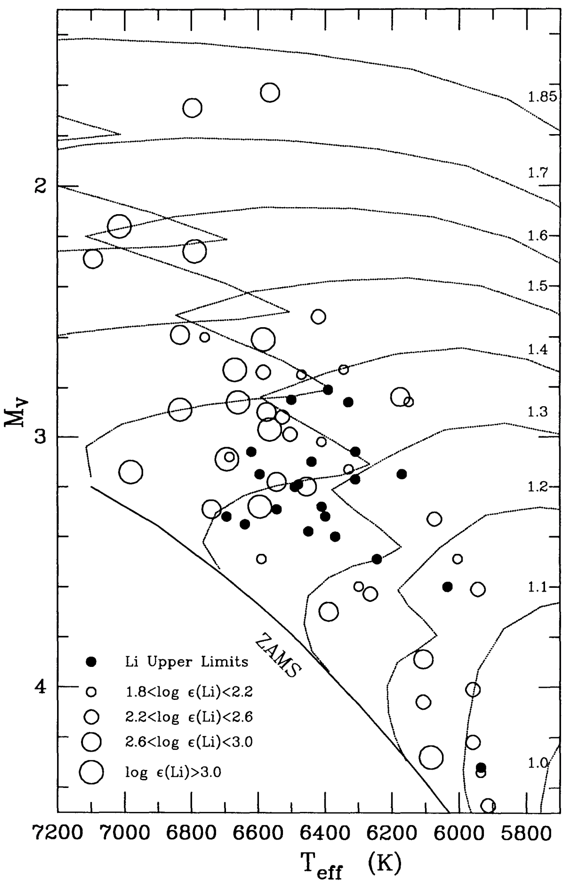

FIG. 8.—Stars from Boesgaard and Tripicco (1986b, 1987) which are not present in our sample are plotted on the H-R diagram. The size of the open circle represents the Li abundance (see key), and the filled circle represents an upper limit. The ZAMS and evolutionary tracks are for [Fe/H] = 0.0 and are taken from VandenBerg and Bridges (1984) and VandenBerg (1985), respectively. Each evolutionary track is labeled in solar masses on the right-hand side of the figure.

H-R diagram. To investigate the effects of metallicity, the sample was divided into three metallicity bins, solar ([Fe/H] > −0.1), intermediate (−0.1 > [Fe/H] > −0.3), and low ([Fe/H] < −0.3), and it was then plotted on the H-R diagram along with the ZAMS (VB) and evolutionary tracks (VandenBerg 1985) for [Fe/H] = 0.0, [Fe/H] = −0.23, and [Fe/H] = −0.46, respectively (Fig. 9). To be consistent with the changes made to the solar metallicity ZAMS and tracks, the lower metallicity ZAMS and tracks have also been shifted to cooler temperatures by 100 K. It is immediately apparent that the Li "dip" does not occur at the same mass at all metallicities. At solar metallicity, the Li-depleted clump is at a mass of around 1.35 $M_\odot$, at intermediate metallicity it is at a mass of around 1.25 $M_\odot$, and at low metallicity it is at a mass of around 1.1 $M_\odot$. This indicates that to first approximation, the "dip" phenomenon is confined to the same effective temperature interval for all metallicities and is not related to the mass of the star.

The mass of each star was determined from the set of evolutionary tracks appropriate to its metallicity, and the main-sequence effective temperature was computed for each mass. In Figure 10, the Li abundances are plotted as a function of the main-sequence effective temperature. The solar metallicity stars have been divided into two groups: those that are below the blueward hook and those that have evolved beyond it. Stars in the region of the hook or at the intersection of a hook and a track of a different mass are not included in either group. Rapidly rotating Li-depleted stars are also excluded. The "dip" is less smeared in the solar metallicity stars which are below the hook (Fig. 10a) than in those that have evolved beyond it (Fig. 10b). The "dip" is also clearer in the stars with the lowest metallicity (Fig. 10d), which contains stars with masses around 1.1 $M_\odot$ that do not go through the hook phase, than in the intermediate metallicity stars (Fig. 10c), which have evolved past the hook. Hence, a large part of the scatter in the "dip" may arise from errors in the mass of the star due to theoretical uncertainty in the position and magnitude of the hook feature. Comparing Figures 10a and 10d, it appears that the center of the "dip" shifts from about 6700 K at solar metallicity to about 6400 K at the lowest metallicity. From the present data, it is not possible to infer if this shift in the "dip" is real or simply an artifact of the theoretical evolutionary tracks used to determine the masses. Observations of a metal-poor cluster in which the "dip" stars are still on the main sequence will resolve this ambiguity and may provide additional clues about the Li depletion mechanism in these stars.

d) Li *Depletion in the* Li-*measured Stars*

Among the stars with measured Li abundances, the range in Li exceeds a factor of 30. We have shown earlier that this variation in Li in each group is not related to the T_{eff} or $v \sin i$ of the star. From our sample, we selected two sets of stars which are in regions of the H-R diagram that are clearly unaffected by the Li "dip." Ag the high-mass end, we have 25 stars with masses greater than 1.5 $M_\odot$ and at the low-mass end, we have 33 stars with masses less than about 1.25 $M_\odot$. The $v \sin i$ and Li abundance distributions in these stars are shown in Figure 11. While the high-mass stars have a large range in rotational velocity between 0 and 100 km s^{-1}, all the low-mass stars are rotating with velocities less than 20 km s^{-1}. The mean Li abundance in the high-mass stars is around 3.0 and that of the low-mass stars is around 2.5. While the distributions are broadened by errors, some of the overlap between the two groups is real; stars with Li abundances between 2.4 and 2.8 are found both at high and low masses. Contrary to earlier understanding, this means that some early F stars with extremely thin convective envelopes which have evolved from main-sequence temperatures greater than 7000 K have managed to deplete their Li by factors of 3–7. Equally interesting is the observation that a few low-mass stars have managed to retain most of their initial Li despite their deeper convective envelopes, while others at the same age have undergone a Li depletion of a factor of 30. The scatter in Li abundances seen in late F stars in young clusters appears to persist in these older stars.

e) *Spectroscopic Binaries*

The presence of a companion star can affect our results in two ways. Additional light will increase the continuum, leading to an underestimation of the equivalent widths and hence the abundances. Also, a nearby companion may alter the rotational velocity of the star which we have assumed is affected by winds and magnetic fields alone. To determine the extent of this effect, it is essential to determine the fraction of stars in our sample that may be spectroscopic binaries. Ten double-lined spectroscopic binaries (SB2) were found among the 199 stars we observed and were discarded from the analysis. These are

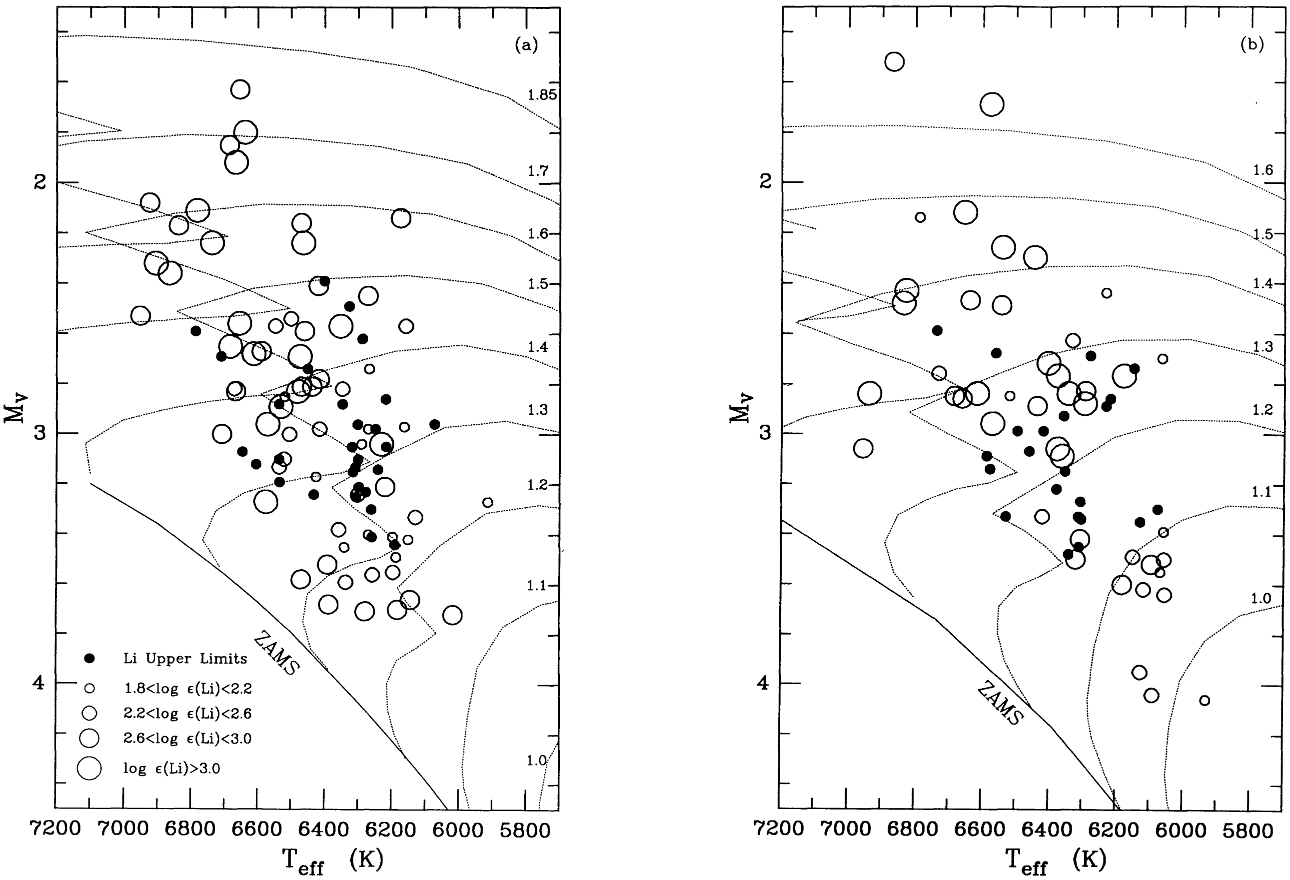

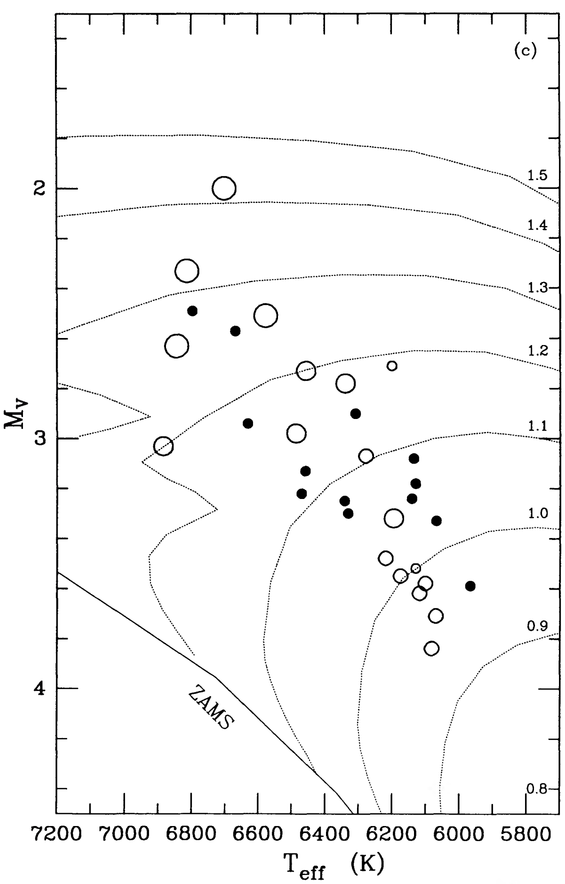

listed in Table 6 along with comments about the relative strengths of the Li lines in the two stars. HR 6493 in particular is very interesting, because the primary is a rapidly rotating F3 star in which the Li line can be clearly seen while the slowly rotating companion is a F6 star which does not exhibit a Li feature and is probably in the Li "dip" (Fig. 1). Several stars are labeled as single-lined spectroscopic binaries (SB1) in the BSC, and these have been identified with a superscript "b" in Table 1. However, selection effects play an important role in determining whether a star has been identified as a spectroscopic binary, and a considerable number of binaries may remain undetected in our sample. Obviously, more luminous companions and short-period binaries can be detected more easily. We used Abt and Levy's (1976) survey (the best available estimate) to determine the number of spectroscopic binaries that may remain unidentified. Out of the 123 F3-G2 stars examined by Abt and Levy (1976), 46 (i.e., 37%) were found to be spectroscopic binaries. Among them, 38 (i.e., 31%) were SB1's and eight (i.e., 6.5%) were SB2's.

In addition to the 10 SB2's we identified, one more is labeled as SB2 in the BSC though it is not obvious in our spectrum. Hence, 11 of the 13 SB2's predicted by Abt and Levy's (1976) statistics have been identified. The known SB1's form only

FIG. 9.—The entire sample is divided into three groups according to metallicity; (*a*) [Fe/H] > 0.1, (*b*) −0.1 > [Fe/H] > −0.3, and (*c*) [Fe/H] < −0.3 and plotted on the H-R diagram. The ZAMS and evolutionary tracks correspond to [Fe/H] = 0.0, −0.23, and −0.46 respectively, and are taken from VandenBerg and Bridges (1984) and VandenBerg (1985). The evolutionary tracks are labeled in solar masses on the right-hand side of the figure. The size of the open circle represents the Li abundance (see key), and the filled circle represents an upper limit.

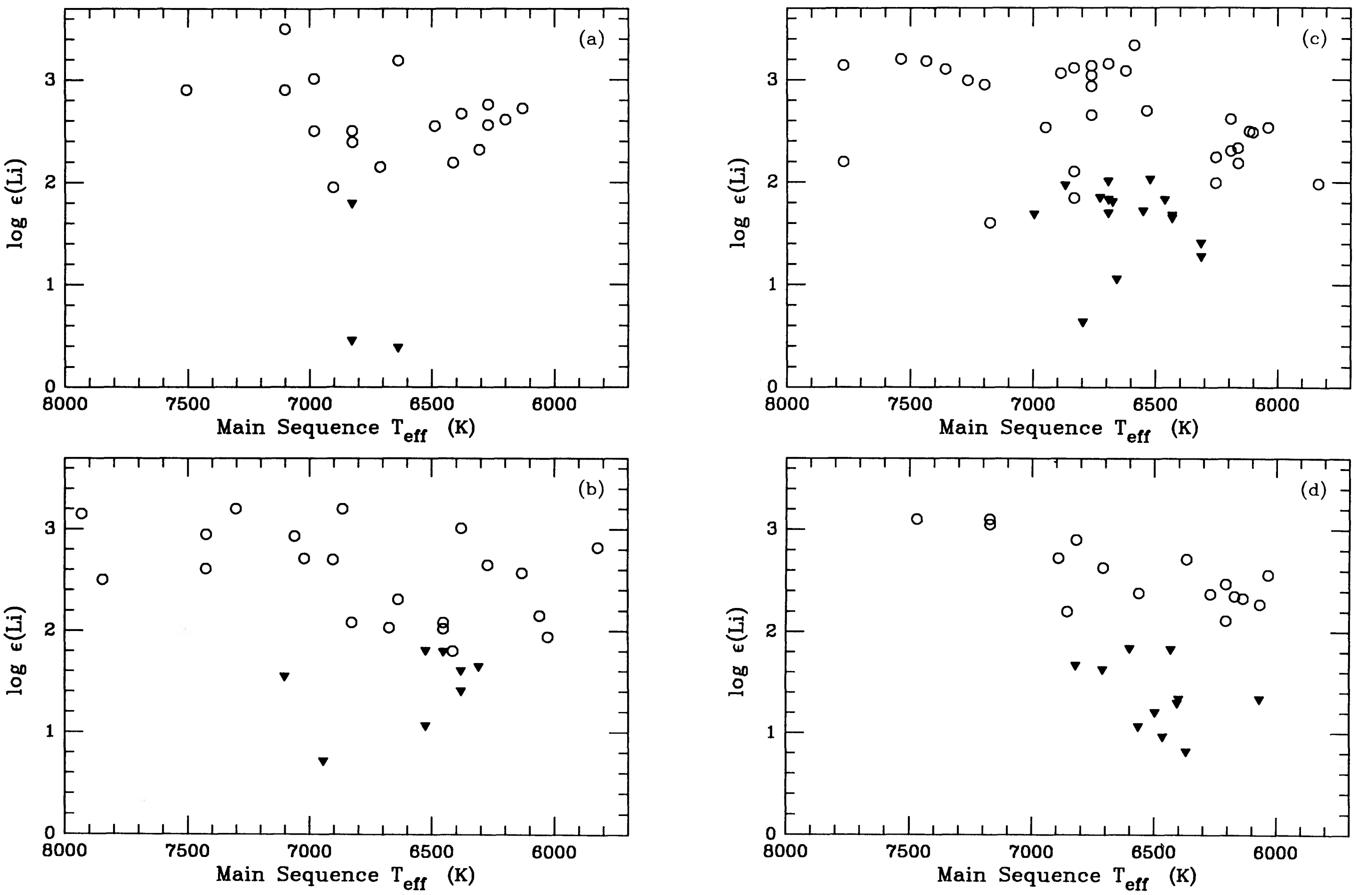

FIG. 10.—Lithium abundances are plotted as a function of the main-sequence effective temperature of the star as calculated from its mass for (*a*) stars with [Fe/H] > −0.1 that are below the blueward hook, (*b*) stars with [Fe/H] > −0.1 that have evolved past the hook phase, (*c*) stars with −0.3 < [Fe/H] < −0.1, and (*d*) stars with [Fe/H] < −0.3.

13% of our sample and, clearly, others must exist if Abt and Levy's statistics are representative. SB1's occur when one component is so much brighter than the other (typically $\Delta m > 2.5$ mag) that it swamps the spectrum of the secondary and renders it invisible. Magnitude differences of 2.5 or greater will increase the continuum and reduce the measured equivalent widths by less than 10%. This has a very small effect on the calculated abundances; a Li abundance of 3.0 will be reduced to 2.95. SB1's may also occur when the secondary is rotating rapidly and its lines are broad and shallow. Three of the SB2's detected in our sample (HR 2962, HR 4570, and 6493) have either one or both stars rotating rapidly. Hence, if a companion is of

TABLE 6

DOUBLE-LINED SPECTROSCOPIC BINARIES

HR Number	Comment
362..........	Both narrow-lined; secondary weaker lines; Li seen in both, weaker in secondary
2236..........	Both narrow-lined; secondary weaker lines; Li not seen in either
2962..........	One narrow, one broad
4230..........	Both narrow-lined; Li weak in both
4822..........	Both narrow-lined; secondary lines weaker; Li not seen in either
4570..........	Both broad-lined; secondary lines equally strong; Li equally strong
5235..........	Both narrow-lined; Li weak in both
5304..........	Secondary not seen
6493..........	One narrow, one broad; Li seen in broad, not in narrow
7955..........	Both narrow-lined; secondary weaker lines; Li not seen in either
8899..........	Both narrow-lined; Li seen in both
8954..........	Both narrow-lined; Li seen in both

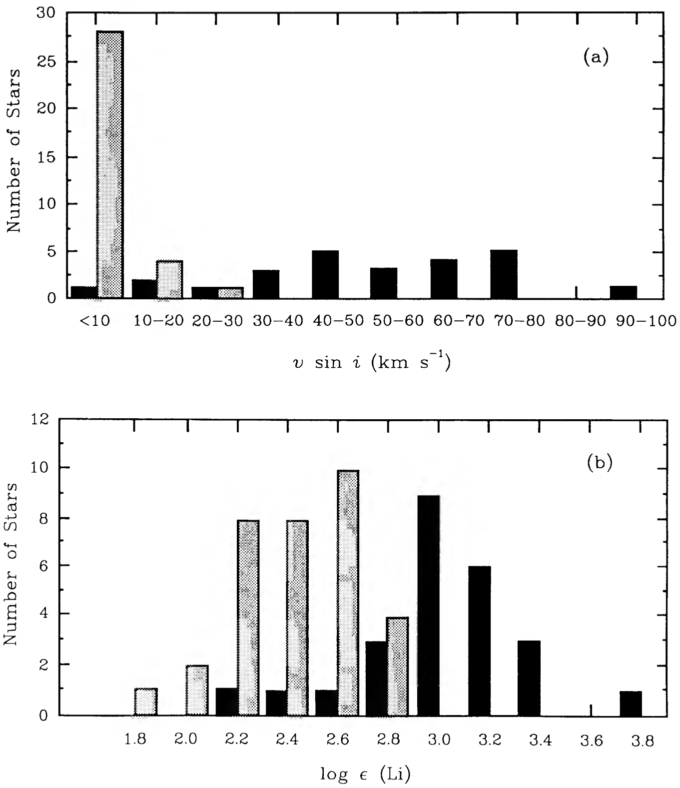

FIG. 11.—(*a*) Projected rotational velocity $v \sin i$ and (*b*) Li abundance distributions in high- and low-mass stars selected on the basis of being removed from and hence unaffected by the Li "dip."

comparable magnitude, it would probably be detected through its double-lined spectrum even if is rotating rapidly. Recall that abundances have been measured in stars rotating as fast as 110 km s^{-1}. Hence, the unidentified SB1's should not have a major impact on the abundance trends observed.

It is more difficult to estimate the effect of low-luminosity companions on the rotational velocity of a star. Some studies have shown that the mass ratio of SB1's peaks around 0.2 while that of SB2's peaks around 1.0 (Trimble 1974, 1978; Staniucha 1979). For our sample, a mass ratio of 0.2 leads to a secondary mass around 0.3 $M_{\odot}$ (a late M dwarf), and it is unlikely that such a secondary could have had a profound influence on the rotational velocity of the F star. There is, however, still some controversy about whether the mass ratio functions are indicative of different physical formation processes for SB1's and SB2's or merely a selection effect. If the companion was about 2.5 mag fainter than the primary as postulated for the marginal SB1, it would be a mid-G star with about half the mass of the primary and could, indeed, have influenced the rotational evolution of the primary star.

V. DISCUSSION

We will discuss several theoretical alternatives that have been proposed to explain the observed Li abundances in stars and attempt to distinguish between those which are still viable and those which are at odds with our observations.

a) Mass Loss

As early as 1965, Weymann and Sears calculated that a mass-loss rate in the Sun about 1000 times larger than the present rate was needed over its entire life to account for the observed Li depletion. Speigel (1967) showed that while mass loss by itself could not account for the depletion observed in the Sun, rotational mixing combined with mass loss may give a reasonable Li-depletion rate. Recently Willson, Bowen, and Struck-Marcell (1987) suggested that very high mass-loss rates ($>10^{-9}$ $M_{\odot}$) are indeed present in stars between 1.0–2.5 $M_{\odot}$ and, in the Sun, this mass loss took place over $\sim 10^9$ years after it arrived on the main sequence; in effect, the Sun has lost one solar mass of matter during its main-sequence life. This mass loss was not proposed to explain the Li abundances in stars but as a consequence of the mass loss, the Li observed in the Sun has to be accounted for; all the material containing Li is removed when a 2 $M_{\odot}$ Sun is stripped of 1 $M_{\odot}$. Guzik, Willson, and Brunish (1987) suggested that the Li observed in the Sun is produced in solar flares by spallation reactions and adopted an energy requirement of 1 erg per Li atom from Ryter *et al.* (1970) to argue for the availability of this energy in solar flares. While Ryter *et al.* acknowledge that this energy is sufficient, they state that ten to hundreds of ergs are necessary in more realistic cases. Spallation reactions produce roughly equal amounts of ^{6}Li and ^{7}Li (Reeves 1974) but the maximum ^{6}Li/^{7}Li ratio observed in meteorites (Krankowsky and Müller 1967) and in stars (Andersen, Gustafsson, and Lambert 1984) is 0.1. Guzik, Willson, and Brunish (1987) suggested that a large part of the ^{6}Li produced in spallation reactions in solar flares was removed by the faster destruction of ^{6}Li. However, if spallation reactions are made to produce the observed ^{7}Li, they will vastly overproduce Be and B. The observed Be and B abundance can be simply accounted for by producing the observed ^{6}Li and about 10% of the observed ^{7}Li in spallation reactions.

The significance of this mass-loss model on our understanding of Li abundances in stars is monumental because we should be looking for ways in which Li can be produced in stars in differing amounts and not for ways in which it can be destroyed. According to the model, the *cosmic* Li abundance seen in early F stars and in meteorites is merely the maximum amount of Li made in flares in stars. Why do all types of stars synthesize Li to the same maximum level? The identical Li abundance seen in young T Tauri stars must then be a coincidence. This maximum Li abundance may no longer be a reflection of the primordial abundance formed in the big bang and cannot be used to constrain models of the universe. However, before this suggestion of extensive mass loss can be considered further, the feasibility of the production of the light elements on stellar surfaces must be addressed in more detail. In addition, there is no observational evidence that such extensive mass loss has indeed taken place, and for the present we will assume that the conventional wisdom on primordial and interstellar Li production holds and attempt to distinguish between the various models put forward to account for its depletion in stars.

b) Convective Overshoot, Microscopic Diffusion, and Meridional Circulation

Calculations involving convective overshoot by Strauss, Blake, and Schramm (1976) were able to reproduce a smooth variation in the Li abundance as a function of mass and age in late type stars. Vauclair *et al.* (1978) accounted for the depletion of Li and the normal abundance of Be in the Sun by varying the extent of overshoot with depth in the star. The same calculations extended to late F stars showed that overshoot was inefficient in stars with thinner convective envelopes. Even if convective overshoot does penetrate deep enough to destroy Li in the late F stars, the efficiency of the overshoot must depend on a third parameter to explain the range in Li abundances in stars of the same mass and age seen in our data. Such a dependence, if invoked, must then be able to produce a range in Li abundance of 1.0 dex in clusters as young as α Per (BLS). Clearly, convective overshoot is not favored to be the primary cause of Li depletion in F stars.

Microscopic diffusion is the result of upward radiative acceleration and downward gravitational force. According to Michaud (1986), Li is pushed upward by radiative acceleration in stars with effective temperatures greater than 6900 K and settles gravitationally in cooler stars. The time scale for gravitational settling increases with the depth of the convective zone (Michaud 1985). Charbonneau and Michaud (1988, hereafter CM) extended the meridional circulation model of Tassoul and Tassoul (1982) to F stars and showed that meridional circulation due to rotation tends to inhibit the diffusion of Li. They calculated that the critical rotational velocity at which meridional circulation becomes more important than diffusion decreases from 50 km s^{-1} at 7250 K to 5 km s^{-1} at 6400 K. At the hotter end of the temperature range, a velocity in excess of the critical velocity should inhibit the overabundance of Li and decrease the Li abundance by circulating the material in the convective envelope to hotter parts of the star. At the cooler end of the temperature range, a velocity in excess of the critical velocity should inhibit the gravitational settling of Li.

As in the case of convective overshoot, gravitational settling may add to the depletion of Li but cannot alone account for the Li abundances seen in the late F stars in our sample. Our data clearly show that Li has been depleted in stars between 6000 and 6400 K, and a large fraction of these are rotating faster than the critical velocity calculated by CM. It is possible that the critical rotational velocities themselves are incorrect; CM state that it remains to be verified that their extension of the radiative rotating models of Tassoul and Tassoul (1982) to F stars with convective envelopes is valid. However, large Li depletions have been reported in the same temperature range in young clusters like the Pleiades (Duncan and Jones 1983) and α Per (BLS) where the time scale for gravitational settling far exceeds the estimated age of the cluster (Michaud 1985).

According to CM, the early F stars in our sample should show signs of Li enhancement if they are rotating slower than the critical velocity. We have adopted the Li abundance log ϵ(Li) = 3.20 as the *cosmic* value on our scale. Four stars in our sample have Li abundances more than 2 σ above this *cosmic* value. The main-sequence effective temperatures from which these stars have evolved (as derived from the evolutionary tracks of VandenBerg 1985) are between 6800 and 7400 K, and their $v \sin i$'s range between 6 and 70 km s^{-1}. Recall that according to CM, the critical rotational velocity varies sharply with effective temperature and, within the errors, it is conceivable that these stars do conform to the model predictions. CM calculated that if all the available Li is pushed into the convective zone, the maximum Li overabundance would not exceed a factor of 8. None of the stars in our sample show such large overabundances. The largest overabundance is a factor of 3.6 in HR 2264. We note that this star is classified as a single-lined spectroscopic binary in the BSC. We concluded earlier that the fainter companion of a single-lined spectroscopic binary probably does not affect the spectrum of the primary; if it has, the Li abundance has been underestimated, and the overabundance is even larger. The companion may also have altered the structure of the star and affected the Li abundance of the primary. We regard the overabundance as extremely interesting but suspect as proof of radiative acceleration. Excluding this star, the maximum Li overabundance is a factor of 2 in HR 5128 and HR 5716. However, several stars with $v \sin i$'s similar to these stars, and in close proximity to them in the H-R diagram, show no sign of Li enhancement, which leads us to believe that the observed enhancement is not significant and may simply be caused by larger errors in a few stars.

At the age of our late F stars (3–4 Gyr), the critical rotational velocity that should bring Li-depleted material to the convection zone by meridional circulation is about 5 km s^{-1} (CM). If the models are valid, the Li depletion observed in the late F stars may be accounted for by such a dilution process. A spread in the initial rotational velocities would then account for the observed spread in Li abundances. The depletion seen in late F stars in young clusters may also be explained by meridional circulation. At the age of the α Per stars, the critical rotational velocity required to contaminate the convective zone of the late F stars with Li depleted material is around 100 km s^{-1}, and such large velocities were indeed seen in several stars in this young cluster (BLS). In this scenario, Li depletion and rotational braking must occur on the same time scale because the Li depleted stars in the young clusters are the slow rotators. However, the early F stars in our sample which have been rotating at similar velocities for 2 Gyr do not conform to the model predictions for meridional mixing. An examination of all the stars in our sample with effective temperatures greater than 6800 K (13 in all) shows no correlation between the Li depletion and $v \sin i$, and there is no indication of Li depletion in some of the most rapid rotators in our sample. Our fastest rotator is HR 3859 with a $v \sin i$ of 100 km s^{-1}. It is presently at an effective temperature of 6640 K but appears to have evolved from a main-sequence temperature of 7000 K. According to CM, Li-depleted material should have reached the convective envelope of this star in a few million years. Instead, HR 3859 has a Li abundance of 3.15 which is equal to the *cosmic* value within our estimated error. Several hotter stars with $v \sin i$'s around 70 to 80 km s^{-1} also show no Li depletion, though the hotter main-sequence temperatures from which they have evolved may mean that they are rotating at velocities lower than their critical velocity. Hence, our observations do not support the meridional mixing calculations of CM, a fact the authors themselves pointed out with the observations that existed previously.

c) *Differential Rotation and Mixing*

Our study of Li depletion in field F dwarfs was designed to look for correlations with rotational velocity and was motivated, in part, by the study of rotation in the Sun by Endal and Sofia (1981). They showed that when a rapidly rotating solar model was spun down by winds and magnetic fields, the outer convective envelope would spin down first while the interior continued to rotate rapidly. Although calculations for Li depletion were not performed, the resulting turbulence was predicted to cause mixing down to depths where the material would be totally Li depleted. Recent calculations by Pinsonneault *et al.* (1989) have extended Endal and Sofia's approach, and the large Li depletion seen in the Sun can be reproduced by the models. Using an initial angular momentum spread of a factor of 10, as derived from the early F stars (Kawaler 1987) which are not expected to have spun down, they calculate the expected range in Li abundance as a function of time starting with a constant *cosmic* abundance. They find that in young stars, differences in the initial rotational velocities do not lead to large differences in the observed Li abundance because though the outer envelope of the initial fast rotator has been spun down, the subsequent mixing has not been completed. However, the spread in Li abundance increases with age as the interior spins down and mixing continues during this process.

The rotational evolution of pre–main-sequence stars is not well understood. However, there is some observational evidence that stars of a given spectral type arrive on the main sequence with a range in rotational velocities (Hartmann and Noyes 1987), and several studies have shown that the distribution of $v \sin i$'s among A and B stars corresponds to a Maxwellian velocity distribution (Deutsch 1970, and references therein). Primarily because of their thinner convective envelopes, early F stars are not expected to spin down on the main sequence. In our data, they are seen with $v \sin i$'s in the range 0 to 100 km s^{-1}, and some of this spread in $v \sin i$ must be intrinsic. The late F stars in our sample are seen to be rotating with $v \sin i$'s between 0 and 20 km s^{-1}. Observations of young clusters (BLS) show a spread in rotational velocities in the late F stars, and it is reasonable to assume (Stauffer 1988) that the late F stars in our sample had an initial spread in rotational velocities similar to that seen now in the ealy F stars. Those late F stars which arrived on the main sequence rotating slowly would not have undergone rotational spin down and the subsequent mixing due to differential rotation. In the absence of alternate ways of depleting Li, these stars should exhibit their initial (i.e., *cosmic*) Li abundance. According to Pinsonneault *et al.* (1989), Li depletion in the late F stars will depend upon the magnitude of the change in the rotational velocity; i.e., stars which were spun down from 100 to 10 km s^{-1} will undergo greater mixing and hence exhibit smaller Li abundances than stars which were spun down from 30 to 10 km s^{-1}. In this scenario, a group of stars which arrive on the main sequence with the same *cosmic* Li abundance and a large range in rotational velocity will be seen to exhibit a large range in Li abundance after they have all spun down. In the absence of correlations with other parameters, mixing caused by differential rotation provides a simple way to account for large variations of the Li abundance in stars which are otherwise similar.

Recall that in the coolest stars in our sample, the maximum Li abundance is around 2.5, a factor of about 5 lower than our adopted value for the *cosmic* Li abundance. This indicates that some depletion has occurred in all the late F stars. It is conceivable that once stars of different initial rotational velocities have spun down and a spread in Li abundances is established, Li depletion continues in all stars by some other process like convective overshoot or gravitational settling which will manifest itself in a few gigayears, the age of our field stars. Such a process will retain the spread in the Li abundances seen in our data while decreasing the average abundance of the sample with age.

If Li depletion is caused primarily by mixing due by differential rotation, the tight Li-$T_{\rm eff}$ relation seen in the Hyades and not in other clusters argues for a small initial rotational velocity dispersion in this cluster alone. We speculate that a small spread in initial rotational velocities may also be responsible for the plateau in Li abundances seen in the halo stars (Spite and Spite 1982; Spite, Maillard, and Spite 1984; Boesgaard 1985; Rebolo, Beckman, and Molaro 1988; Hobbs and Duncan 1987). Though we can offer no evidence for such a notion, we point out that this scenario offers a simple mechanism to produce a plateau starting with the same initial *cosmic* abundance as the Population I stars. The absence of mechanisms that can produce a uniform Li depletion over the observed temperature range is one of the reasons cited for adopting the alternate view that Population II stars started with a lower initial Li abundance.

d) Pre–Main-Sequence Depletion

The modest but real dispersion in Li abundances in the early F stars in our sample remains a puzzle. Although these stars have evolved off the main sequence, they have not evolved far enough toward the giant branch for Li dilution to occur as a result of the deepening convective envelope. According to Iben (1967), a 1.5 $M_\odot$ star must evolve to about 5300 K before its Li is diluted by a factor of 1.5. Some of these stars may have undetected companions that have affected their Li abundances. Our sample contains only 25 early F stars, and the sample must be augmented to evaluate the probability of such an occurrence. In the absence of such effects, it is difficult to explain how stars with thin convective envelopes and no rotational braking can deplete Li on the main sequence. Convective overshoot is extremely improbable in these stars and the only other depletion mechanism, meridional circulation, has been shown to be incompatible with our data. Perhaps the problem lies in assuming that this depletion did occur on the main sequence. Stars which arrive as slow rotators on the main sequence have lost the angular momentum they must have acquired during their contraction onto the main sequence. The process by which they lose their angular momentum (e.g., mass loss) may also lead to some depletion of Li.

There is considerable theoretical uncertainty about the extent of PMS Li depletion. The earliest calculations by Bodenheimer (1965) showed that Li depletion occurred in stars cooler than 6000 K and increased with decreasing temperature. Revised calculations with improved physics showed that no Li depletion occurred in the PMS phase unless "extra mixing" mechanisms were incorporated (D'Antona and Mazzitelli 1984). Recent calculations with increased opacities are able to reproduce the Hyades Li-$T_{\rm eff}$ relation in cool stars with PMS Li depletion alone (Stringfellow, Swenson, and Faulkner 1987, VandenBerg 1989). The rotational evolution of PMS stars is not well understood, and no calculations have been performed to predict the effects of rapid rotation during this phase. Further investigation of Li depletion in the PMS phase, both observational and theoretical, is clearly warranted.

e) Depletion Mechanisms in the Li-*Dip*

Since the first report of the Li "dip" in the Hyades (Boesgaard and Tripicco 1986*a*), the "dip" has been seen in several clusters at least as old as the Hyades; Coma (Boesgaard 1987*b*), UMa stream (Boesgaard, Budge, and Burck 1988), and NGC 752 (Hobbs and Pilachowski 1986*a*; Pilachowski and Hobbs 1988) but is not seen in younger clusters like the Pleiades (Pilachowski, Booth, and Hobbs 1988; Boesgaard, Budge, and Ramsay 1987) and α Per (BLS). It therefore appears that the "dip" forms after the stars have arrived on the main sequence and sometime between 0.07 and 0.6 Gyr.

Two theoretical explanations have been provided for the Li "dip" seen in the Hyades. According to Michaud's (1986) diffusion hypothesis, the Li "dip" reflects the competition between upward radiative acceleration, effective at temperatures greater than 6900 K, and gravitational settling, effective at cooler temperatures. While gravitational settling quickly empties out the shallow convective zone in the "dip" stars, the diffusion time scale for stars at 6400 K is around 10^9 years, providing a plausible reason for such stars in the Hyades to remain undepleted. To account for the absence of Li enhancement in stars hotter than 6900 K, a mass loss of about 10^{-14} $M_\odot$ yr^{-1} was invoked to remove the Li enriched material. While such a mass-loss rate is conceivable, it seems coincidental that the Li abundance after such depletion exactly equals the *cosmic* value.

An alternative to the gravitational settling model is the meridional circulation suggestion of CM. According to this, the "dip" stars in the Hyades have a rotational velocity in excess of the critical rotational velocity and Li has been depleted by meridional circulation. In cooler stars, the lack of Li depletion is explained by the time scale required by meridional circulation to carry matter from the Li-burning region to the convective zone being greater than the age of the Hyades. Our data on early F stars have been shown to be in disagreement with the predictions of the meridional circulation theory. CM cite other objections to their own model, the strongest being that because a scatter is expected in the $v \sin i$–T_{eff} relation in clusters, and the depletion should depend upon the rotational velocity, the "dip" should not be as well defined as seen in the Hyades. Once again, we wonder if the Hyades is not unique in having a small dispersion in rotational velocity. Stars with *cosmic* Li are seen in the region of the "dip" in the UMa stream. These stars have been suspect because of membership and T_{eff} uncertainties but seem to indicate that more detailed investigation of other clusters is needed.

Both theories predict that the Li "dip" should be broader in the older field stars compared to the Hyades, because Li depletion will become more evident in the cooler stars. Small variations in the width of the "dip" are difficult to judge from our sample, but it is clear that the "dip" does not extend much below 6300 K. The smearing of the "dip" is more evident at the high-mass end, and this is probably a result of evolutionary path of the stars. Both theories can be made to account for the presence of some Li-normal stars in the "dip" region. In the diffusion model, Li is merely hidden below the convective zone, where it is supported by radiative forces. The stars in our sample have evolved off the main sequence. If Li survives just below the convective zone, it may mix back into the envelope during the rearrangement of the stellar structure that accompanies hydrogen core exhaustion and subsequent hydrogen shell burning. Alternatively, in the meridional circulation model, the presence of a spread in Li abundances in the "dip" region may be a result of the intrinsic spread in rotational velocities in these stars. Although the "dip" itself can be explained by either theory, our data on the early F stars show serious discrepancies with the meridional circulation models, thus favoring the simpler diffusion hypothesis.

I would like to thank David Lambert for his support and guidance during the progress of this work. I would also like to thank Chris Sneden, Craig Wheeler, and John Scalo for many helpful discussions. The friendly help of the McDonald Observatory staff is much appreciated.

REFERENCES

Abt, H. A., and Levy, S. G. 1976, *Ap. J. Suppl.*, **30**, 273.
Anders, E., and Grevesse, N. 1989, *Geochim. Cosmochim. Acta*, **53**, 197.
Andersen, J. 1980, in *ESO Workshop in Methods of Abundance Determination for Stars*, ed. P. E. Nissen and K. Kjär (Garching: ESO), p. 11.
Andersen, J., Gustafsson, B., and Lambert, D. L. 1984, *Astr. Ap.*, **136**, 65.
Balachandran, S., Lambert, D. L., and Stauffer, J. R. 1988, *Ap. J.*, **333**, 267.
Bodenheimer, P. 1965, *Ap. J.*, **142**, 451.
Boesgaard, A. M. 1985, *Pub. A.S.P.*, **97**, 784.
———. 1987*a*, *Ap. J.*, **321**, 967.
———. 1987*b*, *Pub. A.S.P.*, **99**, 1067.
Boesgaard, A. M., Budge, K. G., and Burck, E. E. 1988, *Ap. J.*, **325**, 749.
Boesgaard, A. M., Budge, K. G., and Ramsay, M. E. 1987, *Ap. J.*, **327**, 389.
Boesgaard, A. M., and Tripicco, M. J. 1986*a*, *Ap. J. (Letters)*, **302**, L49.
———. 1986*b*, *Ap. J.*, **303**, 724.
———. 1987, *Ap. J.*, **313**, 389.
Böhm-Vitense, E. 1981, *Ann. Rev. Astr. Ap.*, **19**, 295.
Bonsack, W. K., and Greenstein, J. L. 1960, *Ap. J.*, **131**, 83.
Butler, R. P., Cohen, R. D., Duncan, D. K., and Marcy, G. W. 1987, *Ap. J. (Letters)*, **319**, L19.
Charbonneau, P., and Michaud, G. 1988, *Ap. J.*, **334**, 746.
Clegg, R. E. S., Lambert, D. L., and Tomkin, J. 1981, *Ap. J.*, **250**, 262.
Collins, G. W., II, and Sonneborn, G. H. 1977, *Ap. J. Suppl.*, **34**, 1977.
Crawford, D. L. 1975, *A.J.*, **80**, 11.
D'Antona, F., and Mazzitelli, I. 1984, *Astr. Ap.*, **138**, 431.
Delbouille, L., Roland, G., and Neven, L. 1973, *Photometric Atlas of the Solar Spectrum from 3000 to 10,000 Å* (Liege: Institut D'Astrophysique).
Deutsch, A. J. 1970, in *Stellar Rotation*, ed. A. Slettebak (Dordrecht: Reidel), p. 207.
Duncan, D. K. 1981, *Ap. J.*, **248**, 651.
Duncan, D. K., and Jones, B. F. 1983, *Ap. J.*, **271**, 663.
Eggen, O. J. 1973, *Pub. A.S.P.*, **85**, 542.
Enard, D., and Anderson, J. 1978, in *Proc. 4th Internat. Colloquium on Astrophyics*, ed. M. Hack (Trieste: Osservatorio Astronomico di Trieste), p. 435.
Endal, A. S., and Sofia, S. 1981, *Ap. J.*, **243**, 625.
Garcia Lopez, R. J., Rebolo, R., and Beckman, J. E. 1988, *Pub. A.S.P.*, **100**, 1489.
Gaupp, A., Kuske, P., and Avda, H. J. 1982, *Phys. Rev. A*, **26**, 3551.
Gray, D. F. 1976, *The Observation and Analysis of Stellar Photospheres* (New York: Wiley).
Guzik, J. A., Willson, L. A., and Brunish, W. M. 1987, *Ap. J.*, **319**, 957.
Hartmann, L. W., and Noyes, R. W. 1987, *Ann. Rev. Astr. Ap.*, **25**, 271.
Hauck, B., and Mermilliod, M. 1980, *Astr. Ap. Suppl.*, **40**, 1.
Hejlesen, P. M. 1980, *Astr. Ap. Suppl.*, **39**, 347.
Herbig, G. H. 1965, *Ap. J.*, **141**, 588.
Hobbs, L. M., and Duncan, D. K. 1987, *Ap. J.*, **317**, 796.
Hobbs, L. M., and Pilachowski, C. 1986*a*, *Ap. J. (Letters)*, **309**, L17.
———. 1986*b*, *Ap. J. (Letters)*, **311**, L37.
———. 1988, *Ap. J.*, **334**, 734.
Holfleitt, D. 1982, *The Bright Star Catalogue* (New Haven: Yale University Observatory).
Holweger, H., and Müller, E. A. 1974, *Solar Phys.*, **39**, 19.
Hunger, K. 1957, *A.J.*, **62**, 294.
Iben, I., Jr. 1967, *Ap. J.*, **147**, 624.
Kawaler, S. D. 1987, *Bull. AAS*, **19**, 1022.
Kraft, R. P. 1967, *Ap. J.*, **150**, 551.
Krankowsky, D., and Müller, D. 1967, *Geochim. Cosmochim. Acta*, **31**, 1833.
Kurucz, R. L. 1979, *Ap. J. Suppl.*, **40**, 1.
Michaud, G. 1985, in *Solar Neutrinos and Neutrino Astronomy*, ed. M. L. Cherry, K. Lande, and W. A. Fowler (New York: American Institute of Physics), p. 75.
———. 1986, *Ap. J.*, **302**, 650.
Nissen, P. E. 1981, *Astr. Ap.*, **97**, 145.
Nissen, P. E., and Gustafsson, B. 1978, in *Astronomical Papers dedicated to Bengt Stromgren*, ed. A. Reiz and T. Andersen (Copenhagen: Copenhagen University Observatory), p. 43.
Olsen, E. H. 1983, *Astr. Ap. Suppl.*, **54**, 55.
Perrin, M. N., Hejlesen, P. M., Cayrel de Strobel, G., and Cayrel, R. 1977, *Astr. Ap.*, **54**, 779.
Pilachowski, C. A., Booth, J., and Hobbs, L. M. 1988, *Pub. A.S.P.*, **99**, 1288.
Pilachowski, C. A., and Hobbs, L. M. 1988, *Pub. A.S.P.*, **100**, 336.
Pinsonneault, M. H., Kawaler, S. D., Sofia, S., and Demarque, P. 1989, *Ap. J.*, **338**, 424.
Rebolo, R., Beckman, J., and Molaro, P. 1988, *Astr. Ap.*, **172**, L17.
Reeves, H. 1974, *Ann. Rev. Astr. Ap.*, **12**, 437.
Relyea, L. J., and Kurucz, R. L. 1978, *Ap. J. Suppl.*, **37**, 45.
Ryter, C., Reeves, H., Gradstajn, E., and Audouze, J. 1970, *Astr. Ap.*, **8**, 389.
Saxner, M., and Hammarbäck, G. 1985, *Astr. Ap.*, **151**, 372.
Sneden, C. 1973, Ph. D. thesis, University of Texas.
Spiegel, E. A. 1967, in *Highlights of Astronomy*, ed. L. Perek (Berlin: Springer-Verlag), p. 261.
Spite, F., and Spite, M. 1982, *Astr. Ap.*, **115**, 357.
Spite, M., Maillard, J. P., and Spite, F. 1984, *Astr. Ap.*, **141**, 56.
Staniucha, M. 1979, *Acta Astr.*, **29**, 587.
Stauffer, J. R. 1988, in *Formation and Evolution of Low Mass Stars*, ed. A. K. Dupree and M. T. V. T. Lago (Dordrecht: Kluwer), p. 331.

Stauffer, J. R., Hartmann, L., Burton, J. F., and McNamara, B. R. 1989, *Ap. J.*, **342**, 285.
Steffen, M. 1985, *Astr. Ap. Suppl.*, **59**, 403.
Strauss, J. M., Blake, J. B., and Schramm, D. N. 1976, *Ap. J.*, **204**, 481.
Stringfellow, G. S., Swenson, F. J., and Faulkner, J. 1987, *Bull.* AAS, **19**, 1020.
Tassoul, J.-L., and Tassoul, M. 1982, *Ap. J. Suppl.*, **49**, 317.
Trimble, V. 1974, *A.J.*, **76**, 544.
———. 1978, *A.J.*, **79**, 967.
VandenBerg, D. A. 1985, *Ap. J. Suppl.*, **58**, 711.
———. 1989, preprint.
VandenBerg, D. A., and Bridges, T. J. 1984, *Ap. J.*, **278**, 679.
Vauclair, S., Vauclair, G., Schatzman, E., and Michaud, G. 1978, *Ap. J.*, **223**, 567.
Vogt, S., Tull, R. G., and Kelton, P. 1978, *Appl. Optics*, **17**, 574.
Wallerstein, G., Herbig, G. H., and Conti, P. S. 1965, *Ap. J.*, **141**, 610.
Weymann, R., and Sears, R. L. 1965, *Ap. J.*, **142**, 174.
Willson, L. A., Bowen, G. H., and Struck-Marcell, C. 1987, *Comments Ap.*, **12**, 17.
Zappala, R. R. 1972, *Ap. J.*, **172**, 57.

SUCHITRA BALACHANDRAN: Institute for Astronomy, University of Hawaii, 2680 Woodlawn Drive, Honolulu, HI 96822